LOW-COST CONTINUOUS PRODUCTION OF CARBON FIBER-REINFORCED ALUMINUM COMPOSITES

A Thesis
Presented to
The Academic Faculty

By

Craig Durkin

In Partial Fulfillment
of the Requirements for the Degree
Master of Science in Materials Science and Engineering

Georgia Institute of Technology

December, 2007

LOW-COST CONTINUOUS PRODUCTION OF CARBON FIBER-REINFORCED ALUMINUM COMPOSITES

Approved By:

Dr. W. Steven Johnson, Advisor
School of Materials Science and Engineering
Georgia Institute of Technology

Dr. W. Brent Carter
School of Materials Science and Engineering
Georgia Institute of Technology

Dr. Joe K. Cochran
School of Materials Science and Engineering
Georgia Institute of Technology

Date Approved: November 12, 2007

ACKNOWLEDGEMENTS

I would very much like to thank Dr. Steven Johnson not only for his advisement and guidance throughout this project, but also for approaching me about working for him in the first place. He gave me an opportunity that I otherwise probably would not have had for continuing my education at such a fine school. His management style, and the camaraderie provided by all of my fellow group members, provided an environment that was at once relaxed and challenging.

Of the many people that made this work possible, probably the most important one is Mr. Rick Brown. He provided thorough training, wrenching, troubleshooting and great conversation throughout the project. His extensive knowledge and creative insight provided clever solutions to many of the fabrication problems encountered during this project. I would also like to thank Dr. Rina Tannenbaum, and her group members Jeremy Walker, Erin Camponeschi, Lex Nunnery, Kit Cantwell, and Larry Pranger for sharing their lab space, training me, and providing good company. Without their support, many of the aspects of this project would have been significantly more difficult. Thanks also go to Dr. Eric Weiser of NASA for donating the carbon fibers that were used in the majority of research.

Finally, I would like to thank my family and friends for providing much stress relief and support throughout my many years at Georgia Tech.

TABLE OF CONTENTS

ACKNOWLEDGEMENTS....iii

LIST OF TABLES....vi

LIST OF FIGURES....vii

LIST OF SYMBOLS AND ABBREVIATIONS....x

SUMMARY....xii

CHAPTER 1. INTRODUCTION....1

CHAPTER 2. BACKGROUND....3
2.1 Difficulties associated with composite production....5
2.1.1 Poor wettability....6
2.1.2 Interfacial reaction....11
2.1.3 Thermal stresses....13
2.2 Manufacturing of composites....15
2.2.1 Squeeze casting....16
2.2.2 Ultrasonic infiltration and gas pressure infiltration....18
2.2.3 Gas Pressure Infiltration....22
2.2.4 Alloying Additions....25
2.2.5 Fiber Coatings....27
2.2.5.1 Metallic coatings....28
2.2.5.2 Fluoride salts....30
2.2.5.3 Ceramic coatings....32

CHAPTER 3. OBJECTIVES....37
3.1 Develop a fiber coating....37
3.2 Develop manufacturing technique....39

CHAPTER 4. RESULTS....40
4.1 Zirconia coating....41
4.2 Alumina coating....45
4.3 Composite Fabrication....48
4.3.1 Fiber “Sandwiches”....49
4.3.2 Fiber Dipping and Drawing....50
4.3.3 Squeeze-Casting of Composite Samples....52
4.3.4 Ultrasonic Infiltration of Aluminum in to Carbon Fiber....55
4.4 Tensile Testing Results and Discussion....57
4.4.1 Strength data....59

4.4.2 SEM analysis.....61
4.5 Carbon coating.....70
4.5.1 Coating and testing procedure.....74
4.5.2 Coating results.....76

CHAPTER 5. CONCLUSIONS.....89

CHAPTER 6. RECOMMENDATIONS.....90

REFERENCES.....92

LIST OF TABLES

Table 1: Average mechanical properties of several composite specimens.....60

LIST OF FIGURES

Figure 1: Profile view of molten aluminum on a carbon substrate indicating the wetting angle.....9

Figure 2: Idealized cross-section of a composite.....10

Figure 3: Thermal stresses as predicted by two different models.....14

Figure 4: Squeeze casting process.....17

Figure 5: Schematic of ultrasonic infiltration process. 19

Figure 6: SEM micrograph of a composite sample broken in tension.....21

Figure 7: Precursor filament production using gas pressure infiltration.....23

Figure 8: Variation of contact angle with temperature for a sessile drop of aluminum on a pyrolytic carbon substrate.....31

Figure 9: Variation of mean tensile strength of extracted carbon fibers with molten aluminum contact time.....32

Figure 10: TGA trace revealing weight loss of sized fibers near 380°C.....40

Figure 11: Zirconia crystals.....42

Figure 12: Presence of zirconium as confirmed by the Hitachi S-800 EDX detector.....42

Figure 13: Cracked zirconia coating from 2.5% solution on IM7 fiber.....44

Figure 14: Top-down transition from "ambiguously perfect" to cracked coating.....45

Figure 15: 1:100 dilution of original aluminum oxide solution.....47

Figure 16: 1:125 dilution of the original aluminum oxide solution.....47

Figure 17: Fiber sandwich after emerging from the furnace.....50

Figure 18: IM7 Fibers with poorly-adhered aluminum layer. No infiltration.....51

Figure 19: Pellet produced by applying pressure between aluminum oxide tubes.....53

Figure 20: Stainless steel squeeze casting fixture.....54

Figure 21: Leaking of metal from the squeeze casting fixture.....55

Figure 22: Polished cross-section of composite with aluminum oxide-coated fibers.....59

Figure 23: Broken composite samples mounted in copper tubing.....59

Figure 24: Fracture face of G30/Al composite sample broken in bending.....62

Figure 25: Fracture face of composite sample at 30° angle.....62

Figure 26: Well-infiltrated fibers in Al-IM7 composite sample.....63

Figure 27: Void region in coated fiber composite.....64

Figure 28: Al-IM7 composite cross-section. White regions represent void areas.....65

Figure 29: 24k tow of G30 fibers infiltrated with aluminum.....65

Figure 30: Identical fibers: Al_2O_3-coated on the left, plain IM7 on the right.....66

Figure 31: Coated fiber in void region.....67

Figure 32: EDXS spectra of: 2) fiber coating 4) bulk matrix.....68

Figure 33: EDXS spectra of: 1) fiber coating 2) fiber along its axis 3) matrix pulled away from fiber. Each fiber diameter is 5.2μm.....69

Figure 34: Common graphite plane orientation in fibers: radial, random, onion skin.....71

Figure 35: Amorphous carbon coating deposited by asphalt-toluene solution.....72

Figure 36: Fractured IM7 fibers and their points of convergene for graphite planes.....73

Figure 37: Schematic illustrating possible arrangement of graphite planes.....73

Figure 38: End of composite sample with asphalt-coated fibers.....75

Figure 39: Fibers coated with asphalt solution with no subsequent pyrolysis.....76

Figure 40: Asphalt-coated fibers pyrolyzed at 300°C.....77

Figure 41: Asphalt-coated fibers pyrolyzed at 550°C.....77

Figure 42: Asphalt-coated fibers pyrolyzed at 800°C.....78

Figure 43: Fibers that have undergone the coating/pyrolysis process twice.....79

Figure 44: Variance in fiber diameter.....80

Figure 45: Fracture face of broken composite sample with asphalt-coated fibers.....81

Figure 46: Fracture face with bubble area removed.....81

Figure 47: Composite fracture face with void regions removed.....83

Figure 48: Fracture face detail, showing stronger fiber/matrix interface.....84

Figure 49: Transverse cracking in asphalt-coated fiber composite.....85

Figure 50: Detail of transverse cracking in asphalt-coated fiber composite.....85

Figure 51: Coated fibers at the edge of a bubble.....87

Figure 52: Fibers at the edge of bubble.....87

Figure 53: Detail of cracked and partially removed aluminum oxide coating from asphalt-coated fiber.....88

LIST OF SYMBOLS AND ABBREVIATIONS

% w/v	percent weight per volume
% ROM	percent rule-of-mixtures properties
°C	degree Celsius
°K	degree Kelvin
3K/6K/...	3,000 or 6,000 filaments per fiber
A	amplitude (m)
at. %	atomic percent
c	propagation velocity (m/s)
CTE	coefficient of thermal expansion
CVD	Chemical Vapor Deposition
dA	unit area (m^2)
D_f	driving force (J/m^2)
EDX(S)	Energy Dispersive X-Ray (Spectroscopy)
GPa	gigapascal ($1x10^9$ N/m^2)
kHz	($1x10^3$ per second)
kPa	kilopascal ($1x10^3$ N/m^2)
ksi	1,000 lbs/in^2 (psi)
MMC	metal matrix composite
MPa	megapascal ($1x10^6$ N/m^2)
nm	nanometer ($1x10^{-9}$ m)

OSHA	Occupational Safety and Health Administration
PAN	polyacrylonitrile
p_m	acoustic pressure (N/m^2)
ppm	parts per million
r	pore radius (m)
ROM	Rule of Mixtures
SEM	Scanning Electron Microscope/Microscopy
t	time (seconds)
TGA	Thermo-Gravimetric Analysis
vol. %	volume percent (volume fraction * 100)
wt. %	weight percent
γ	surface tension (J/m^2)
ΔP	pressure (N/m^2)
η	viscosity (poise)
θ	contact angle (degrees)
μm	micrometer ($1x10^{-6}$ m)
ρ	density of the medium (g/cm^3)
ω	angular frequency (radians/s)

SUMMARY

Carbon fiber-reinforced aluminum composites were researched because of their potential to serve as structures that provide several advantages over the traditional manifestations of carbon fiber and aluminum, namely polymer-matrix composites and aluminum alloys, respectively. Carbon fiber-reinforced aluminum would be able to operate in several environments unsuitable for traditional polymer matrix composites, owing to the high melt temperature and high environmental resistance of the aluminum matrix. Such metal matrix composites could be used in high temperature (> 300°C) or especially corrosive environments, for example. These composites would also possess several benefits over standard aluminum alloys, as the fibers have very high specific strength, and could produce aluminum-matrix composites with higher strength-to-weight ratios than present-day alloys. Additionally, since the fibers also have a zero axial coefficient of thermal expansion, they provide the possibility of reducing aluminum's high coefficient of thermal expansion for applications requiring dimensional stability and light weight, such as outer space structures.

The fabrication of carbon fiber/aluminum composites is fraught with problems. Aluminum and carbon do not wet one another, so the liquid metal will not spontaneously flow within the interstices of a carbon fiber tow. The application of pressure is usually required as a means of inducing infiltration, and this can complicate design significantly. Aluminum and carbon can also react with one another to produce the undesirable aluminum carbide, so contact time between the molten metal and the fibers must be

limited. Finally, aluminum and carbon can form a galvanic couple if exposed to mobile electrolyte, so care must be taken in production to shield interfaces from the environment.

Fabrication is usually conducted through pressure-assisted casting, or with the use of ultrasound to induce cavitation and encourage infiltration. Very often these methods are combined with fiber coatings that are designed to improve the fibers' wettability and protect the fiber from any harmful reaction with the aluminum. However, since a large portion of the research into composite fabrication was conducted at a time when carbon fibers were much more expensive, little emphasis was placed on economical means of manufacture or coating.

The research conducted in this study was concerned with the development of low-cost continuous production of carbon fiber/aluminum composites. Two coatings, alumina and zirconia, were applied to the fibers using a sol-gel method and common metal salts. A third coating, an amorphous carbon coating derived from asphalt, was pursued as a means of improving the adhesion of the oxide coatings to the fibers. All fibers were infiltrated with molten aluminum using an ultrasound sonicator, allowing for continuous production and obviating the need for developing heavy tooling to withstand a high gas or mechanical pressure.

The composites produced with ultrasound were well-infiltrated, and were tested in tension to determine their mechanical properties. In general these were quite poor, with strengths being only 15-35% of the theoretical values predicted by the rule of mixtures. Their microstructure revealed a sizable void fraction and the fibers within the composites did not contain any coating on their surface. It was hypothesized that this was a result of few exposed graphite plane edges on the fiber surface, making the fiber nonreactive to

the oxide coatings. To improve the fiber reactivity, an amorphous carbon coating was applied to the fiber surface, but still the oxide coatings were removed from the fibers upon infiltration. It was found, however, that the carbon coating on its own did strengthen the interface between the fiber and the aluminum.

1. INTRODUCTION

The general appeal of composite materials stems from the fact that most monolithic materials excel in only a few areas, such as hardness, refractoriness, cost, toughness, ease of processing, etc. Composite materials are developed in order to obtain combinations of mechanical, thermal, or electrical properties that would otherwise not be feasible. These “unnatural” groups of properties exist through a principle known as the rule of mixtures (ROM). It states that the properties of a composite material are a weighted average of the properties of its constituents. This is a somewhat intuitive statement: if a composite is made of two components in equal parts, it is logical to assume that many of its properties will be an average of the components’.

The power of this principle comes from component proportion and component selection. By altering what the composite is made of, and in what quantities, its properties can be specifically tailored for a desired application. Many of the monolithic materials that originally prompted composites research can find new utility as composite phases, as their shortcomings can be overcome by appropriately pairing each component with another that complements its properties.

Most fiber-based composites operate on this principle, for although today's reinforcing fibers can be of extremely high strength and stiffness, their small size and brittle nature makes them unsuitable for reinforcing applications as-is. These fibers are thus paired with a polymer or epoxy matrix, which on its own is very light and very

tough, but not particularly strong. With each joined as a composite material, they form a material that has excellent strength and toughness properties.

The research conducted in this study specifically concerns the development of low-cost, durable aluminum/carbon fiber composites. Composites made from these constituents have great potential, as both aluminum and carbon fiber are already in many high-performance applications. Their union would provide distinct advantages where each single constituent would be lacking.

2. BACKGROUND

To evaluate how carbon fiber/aluminum composites would improve over traditional aluminum alloys, one can consider the fibers as a carbon alloying addition. Two metal-based materials that rely heavily on carbon as an alloying addition are the metal carbides and the carbon steels. In comparing metals to their carbide, or low-carbon steels to high-carbon steels, one can identify a general trend of increased carbon content causing increased strength, increased modulus, improved hardness/wear, and increased brittleness. This trend is carried forth in the addition of carbon fibers to aluminum. Carbon fiber-reinforced aluminum should be much stronger and stiffer, as well as display better wear properties at the expense of reduced toughness.

Carbon fiber-reinforced aluminum would not only possess significant strength improvements over aluminum alloys (according the rule of mixtures), but also such composites would possess significant improvements in specific strength as well, owing to carbon fiber's strength-to-weight ratio of at least 10 times greater than that of common engineering aluminum alloys. Fiber addition would impart significant stiffness gains to the aluminum, which has a modulus near 72 GPa, while the fibers possess a modulus between 290-530 GPa.

Fiber reinforcement can also impart significant dimensional stability to aluminum alloys, as the fibers have a neutral or slightly negative coefficient of thermal expansion. Dimensional stability is a key criterion for any structure operating over a range of temperatures, such as structures operating in outer space. Such areas of application have

largely been off-limits to aluminum alloys, owing to their rather high coefficient of thermal expansion (CTE) of 22-25 ppm/°K.

Compared to polymer matrices within which carbon fibers are usually bound, aluminum alloys offer several advantages. While it is true that aluminums are stronger and stiffer than polymer matrices, the strength differences between the two would likely result only in better transverse properties of the composite, whereas stiffness differences may make processing of aluminum-matrix composites more difficult. The greatest gains realized from using an aluminum matrix over a polymeric matrix are in the areas of durability and environmental resistance.

Polymer matrices are susceptible to several varieties of environmental attack, including attack by oxidation, corrosion, radiation, moisture, and fire. Fire resistance is especially poor; in addition to their low usage temperature, many matrices are thermosetting, and fire exposure will cause them to burn and emit noxious fumes rather than melt. An aluminum matrix is substantially more resistant to these degradation processes, and can withstand temperatures up to 340°C before beginning to anneal [1].

The final factor making aluminum-carbon fiber composites desirable is cost. The price of carbon fiber is such that it is no longer solely the domain of high-dollar aerospace projects. Rather than $1500 / lb, fibers with excellent properties can be purchased for $15 / lb, and these fibers are in high demand from military, aerospace, and sporting goods projects the world over. The demand for fibers is so great that the research conducted in this project was hindered for some time from inability to procure any fibers.

2.1 Difficulties associated with composite production

Despite the numerous potential advantages over traditional composites or alloys, metal matrix composites as a class of materials are difficult to manufacture. This is especially so with an aluminum matrix. The foremost factors to address in fabricating metal matrix composites are the high melt temperature of the matrix and the inherent stiffness of the matrix as compared to a polymer matrix.

One common technique for fabricating complex-shaped parts with polymer matrix composites is to use a material known as a "prepreg" - a mat of woven carbon fiber pre-impregnated with an appropriate amount of uncured epoxy. After forming to the desired shape, the prepreg is cured and the composite is produced. Composites created in this fashion do not suffer significant losses in mechanical properties because the matrix is not stiff; undulating woven fibers are able to straighten under load.

Metal matrices, however, are significantly stiffer than their polymer counterparts. Aluminum's modulus of 72 GPa is close to 25 times greater than that of most epoxies [1]. Curved or bent fibers in aluminum will break before being able to straighten and bear their full load [2]. Furthermore, metals do not undergo any type of cure cycle. They flow only at temperatures very close to their melt temperature, which is 660°C for aluminum. Such high temperatures impose costs and limitations on the type of processing techniques available. Typically, large-scale aluminum-matrix composites are produced using "precursor filaments." A precursor filament is a single fiber tow that has been infiltrated with aluminum. It can be considered as a one-dimensional analog to prepreg. Such

filaments can be laid up in mats, bent to form curved shapes, or pultruded to form tubing [2].

An additional drawback of aluminum as a matrix material is that aluminum is an exceptionally strong oxide-former. It will possess a thin, inert, protective oxide layer on any free surface, even in the best of vacuum conditions. Debate continues in the literature [3][4][5] regarding the nature of interactions between aluminum metal and aluminum oxide because of uncertainty as to if the metal surface is truly oxide-free. For non-theoretical purposes, any surface of aluminum, in solid or liquid phase, can be considered as oxidized to some extent. As mentioned above, aluminum is resistant to many degradation processes, and much of this resistance derives from the protective oxide scale. The drawback of the surface oxide is that it can interfere with processing of the composite, since it acts to passivate the surface of the metal and impede further chemical interactions.

2.1.1 Poor wettability

The addition of carbon fiber to aluminum presents several additional problems arising from interactions between the two. Prior to immersion in the aluminum melt, the most pressing concern is oxidation of carbon fiber to carbon dioxide and carbon monoxide at 500°C unless atmosphere is controlled [6]. Once the fibers are in the melt oxidation is unlikely, but several incompatibilities between the two components become relevant. The largest of these incompatibilities is that they do not wet one another.

Wetting is a term that describes the contact between a liquid and a solid surface. The amount of wetting is controlled by the thermodynamic tendency to minimize free energy. Atoms at surfaces possess higher energy because they have unsatisfied coordination numbers. They are attracted inward by atoms in the bulk of the material, but by nature of being a surface, there are no atoms available to exert an outward force on the surface atoms and cause the net force to be zero. As a result, surface atoms exert stronger attractive forces on their surface neighbors, giving rise to surface tension. Surface atoms are also in a state of compression and therefore creating new surface (moving additional atoms to the surface) requires the work $\gamma * dA$ for each dA of surface area created. The surface tension, γ, is expressed as energy per unit area, such as mJ/m^2. Liquids, with their ability to flow, can adjust their surface area and respond to these energetic demands by compressing themselves and minimizing surface area. Solids, unable to change their surface area, do still possess surface tension but it is defined in more abstract thermodynamic terms, since it is experimentally harder to verify the work necessary to stretch a solid surface [7].

The extent of wetting on a solid-liquid interface, such as molten metal in contact with carbon fibers, can be described qualitatively through considering the two processes at work: liquid and solid each trying to minimize its respective free energy. The liquid droplet will not spread significantly over the solid surface if the solid surface tension cannot balance the compressive forces on the liquid surface; the liquid will maintain itself compressed in to a droplet. Likewise, the solid, being unable to flow and adjust its surface area, can only reduce its free energy by covering its surface with something of a

lower surface tension. These concepts can be described quantitatively through the Young-Dupré equation [7]:

$$\gamma_{LV} \cos \theta = \gamma_{SV} - \gamma_{SL}$$

where γ denotes surface tension, and the subscripts L, S, and V denote liquid, solid or vapor. θ is the contact angle between solid and liquid. Contact angle is a metric for the degree of wetting. A liquid is considered to wet a solid for $\cos \theta > 0$, or when $\gamma_{SV} > \gamma_{SL}$. In that situation, the solid would "prefer" to form interfaces with the liquid over the vapor, since coverage by a liquid would lower the free energy of the solid by $(\gamma_{SV} - \gamma_{SL})^* dA$.

Liquid aluminum will form a droplet of contact angle nearing 160° on a carbon surface at 700°C [8]. $\cos 160° \approx -0.93$, so such an angle is indicative of extremely unwetting behavior. This behavior is visible in Figure 1. It illustrates a sessile-drop experiment conducted for the purpose of determining contact angle and wetting characteristics.

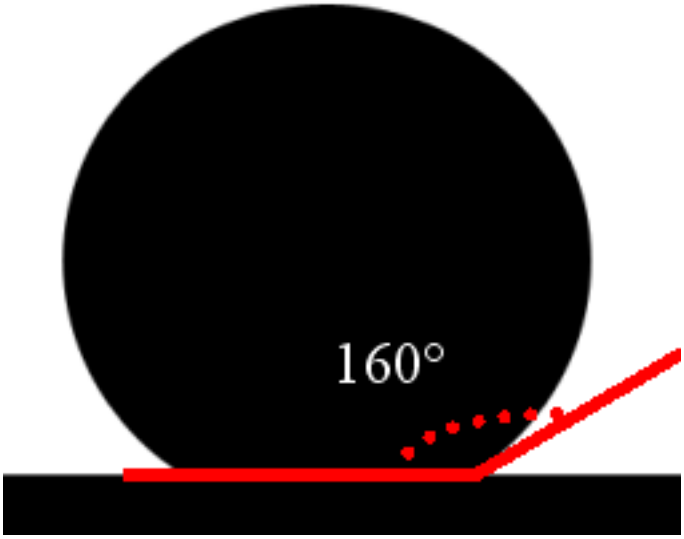

Figure 1: Profile view of molten aluminum on a carbon substrate indicating the wetting angle. Adapted from [8].

The impact of this is probably best illustrated by considering that in order to produce a composite of even a modest volume fraction of carbon fibers, aluminum needs to flow into several thousand individual filament interstices, each only several micrometers wide. This is depicted below in Figure 2. The figure shows an idealized cross-section of a composite, with the fibers marked as dark circles, and aluminum filling fiber interstices which can be considered units of area A. For fibers of diameter 7 μm and fiber volume fraction of 0.2, area A is 154 μm^2, the equivalent of a circular pore of radius 7 μm.

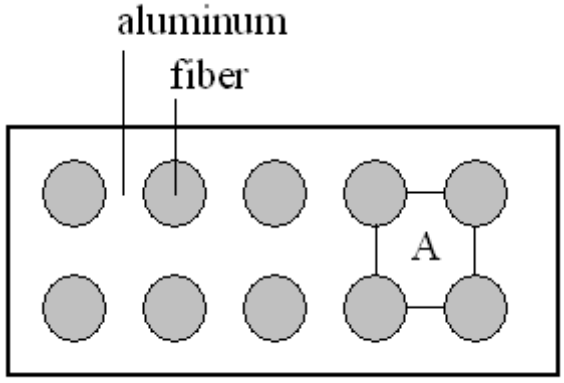

Figure 2: Idealized cross-section of a composite. Aluminum fills the fiber interstices of area A.

With the wettability of the components being so poor, fabrication of aluminum/carbon fiber composites tends to require the assistance of some outside pressure. It can be shown [7] that a pressure ΔP will force the molten metal to infiltrate a pore of radius r according to:

$$r = -2\, D_f / \Delta P$$

where D_f is the driving force for wetting, defined as:

$$D_f = \gamma_{LV} \cos \theta$$

For aluminum, $\gamma_{LV} = 1050$ mJ/m^2 and $\theta \approx 160°$. In the case of pores of radius 7 μm as described in Figure 2, ΔP is 281 kPa. However, fluid viscosity requires that pressure to be maintained for a certain period of time in order achieve full infiltration. Distance infiltrated in to the pore, x, is represented as [7]:

$$x = \left[\frac{r^2 t}{4\eta}\left(\Delta P + \frac{2D_f}{r}\right)\right]^{1/2}$$

where r is the pore radius, t is time, and η is the fluid viscosity.

For pores of radius 7 μm under pressure of 1 MPa, much more than the 281 kPa necessary simply to infiltrate, the liquid metal will advance 9.7 cm / s. However, these values are theoretical calculations, calculated at a low volume fraction. Pressure values in the literature are typically an order of magnitude higher. Girot [9] has shown that this is to prevent solidification of the aluminum metal as it advances into reinforcing fibers, as they are often preheated only to around 500°C [10], while the aluminum is usually heated to 800°C to increase its fluidity. Higher pressures can also be necessary if the fibers have adsorbed gases or particulate matter that needs to be displaced.

Composite production is thus significantly more difficult when the components do not wet one another, as application of pressure to molten metal limits design options and increases cost and design time. Additionally, even if composite production is successful, it is possible that the interface between fiber and matrix will be so poor as to hinder load transfer and severely affect transverse properties.

2.1.2 Interfacial reaction

The statement that carbon and aluminum poorly wet one another carries with it a certain assumption of time. If carbon and aluminum are maintained in contact with one another for several minutes, contact angle between them will decrease. This is because a chemical reaction can occur between carbon and aluminum resulting in the formation of

aluminum carbide, Al_4C_3. Aluminum carbide is mutually wetting of both aluminum and carbon. This reaction can occur at any temperature above 550°C [11], but is seen especially above 900°C where Al_2O_3 decomposes to Al_2O vapor, and the reaction likely occurs at a faster rate [8].

Aluminum carbide is a brittle, hygroscopic ceramic [12]. These characteristics make it an undesirable byproduct of composite processing; high carbide concentration drastically undermines the mechanical properties and longevity of the composite. Aluminum carbide's hardness and brittleness means that it acts as a stress concentrator, and that it fails at fairly low strain. Li and Chao [10] reported that composites heat treated at 600°C to encourage carbide formation experience a direct loss of composite strength with heat treatment time. As-cast composites possessed 32.5% rule-of-mixtures strength, while those heat-treated for 60 hours possessed only 6.9%. Aluminum carbide's hygroscopic nature ensures that the composite will swell and crack if the fiber/matrix interface is exposed to moisture. Traditional methods of avoiding carbide formation have been through the use of fiber coatings, less reactive fibers, or manufacturing processes that limit the amount of time fiber is in contact with molten metal.

Although these composites excel in several areas of environmental durability, they are potentially vulnerable to galvanic corrosion to the extent that the fiber/matrix interface is exposed to a mobile electrolyte. In that situation, carbon and aluminum form a strong galvanic couple, with aluminum being strongly anodic and carbon being slightly cathodic. There is, however, little practical reason why one would want exposed interfaces.

2.1.3 Thermal stresses

One final complication resulting from composite manufacturing is the differing coefficients of thermal expansion of the fiber and matrix. Carbon fibers tend to have neutral or slightly negative coefficients of thermal expansion along their axis, and a moderate CTE of 6-9 ppm/°K in their transverse direction. Aluminum is an isotropic material, and possesses a CTE of 22-25 ppm/°K in all directions. Since the composites have to be processed at elevated temperatures, thermal stresses are going to arise once the matrix has cooled enough to be unable to recrystallize dislocations. As stated before, this temperature is about 340°C.

Two popular models for predicting the thermal stresses in a cooling composite are the Cox model [13] and the Vedula model [14]. Each predicts residual thermal stresses according to differences in CTE of the components. In Figure 3 are the radial (those directed along the fiber radius) and hoop (those acting about the fiber circumference) stresses predicted by each model for an aluminum-carbon fiber system cooled from approximately 340°C to room temperature. The y-axis displays magnitude of residual stress, with negative stresses being compressive in nature. The x-axis displays distance along the fiber-matrix interface as a fraction of the fiber radius: 1.00 on the x-axis is exactly at the fiber matrix interface, while 1.4 is a distance 0.4 fiber radii into the aluminum.

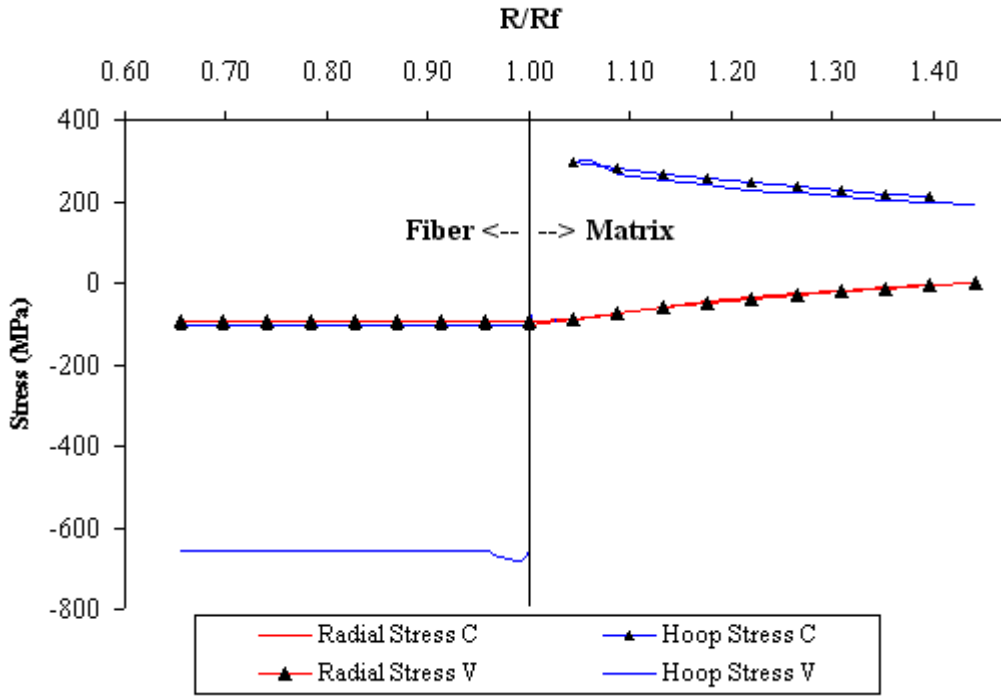

Figure 3: Thermal stresses as predicted by the Cox model (C) and the Vedula model (V)

The numbers are clearly theoretical, as pure annealed aluminum will yield at 34 MPa, and this will limit the magnitude of stresses achievable. Axial stress is not included in this graph because the fibers are significantly stronger than the metal, and the 34 MPa limit imposed by the aluminum is not a significant fraction of the fiber strength. Hoop and radial stresses are shown because both are strongly compressive in the fiber region. This could have the effect of creating a very strong fiber-matrix interface, as the matrix is essentially "choking" the fiber. Such a strong interface is not necessarily desirable, as one means of dissipating energy in composites is through fiber pull-out – a frictional resistance generated by physical sliding of fibers within the matrix under load. If the interface between fiber and matrix is too strong, the fibers will be unable to pull-out and the composites may break at a low stress. Also, such an interface is only physical in

nature; it bears no relevance to the quality of the interface with regard to degradation or other chemical interactions that occur during fabrication.

2.2 Manufacturing of composites

Despite some problems, several compelling reasons do remain for pursuing aluminum/carbon fiber composites, and correspondingly, several attempts have been made towards their realization. Aluminum/carbon fiber composites present both manufacturing problems and chemistry problems, and the breadth of issues to be addressed has allowed for several creative approaches in development of functional materials. Unfortunately, even after several decades of research, there is only a knowledge base of limited value. Some studies produce composites with near rule-of-mixtures properties while addressing production from a manufacturing standpoint only – that wetting problems can be managed through application of pressure, and that interfacial reactions can be controlled through limiting component exposure time. Others produce high quality composites by addressing these problems through chemical means, such as protective fiber coatings, wettability-enhancing fiber treatments and alloying additions. Still other studies apply a combination of both approaches. The result is a large amount of knowledge regarding which specific setups and conditions have worked in the past, but with little information regarding which factors are contributing to that success. Nevertheless, a survey of past work is useful, if for nothing more than developing trends and eliminating processes that would be too costly or time-consuming. What follows is

an overview of common manufacturing processes and chemical alterations used in the production of aluminum/carbon fiber composites.

For reasons described previously, manufacture of aluminum-matrix composites is dominated by pressure-assisted processes. Regardless of what fiber treatment or alloying addition is used, fabrication will likely involve one of three processes: squeeze casting, ultrasonic infiltration, or gas pressure infiltration. The particular process used depends on the shape being produced. Squeeze-casting is used for thick, complex parts, while ultrasonic infiltration is used for parts with thin walls and/or high surface area such as tubes or sheets. The third process, gas-pressure infiltration, whereby a pressurized gas substitutes for a hydraulic ram or ultrasonic transducer, is applicable to both scenarios.

2.2.1 Squeeze casting

Squeeze-casting is a process that was originally developed in Russia in the late 19th century. It is different from standard casting through its use of a hydraulic ram to pressurize the cast material as it solidifies. The application of pressure eliminates pores and air gaps in the material, resulting in better heat transfer and faster cooling rates, and in turn, finer grain size and better mechanical properties [15]. A schematic of the process is visible in Figure 4.

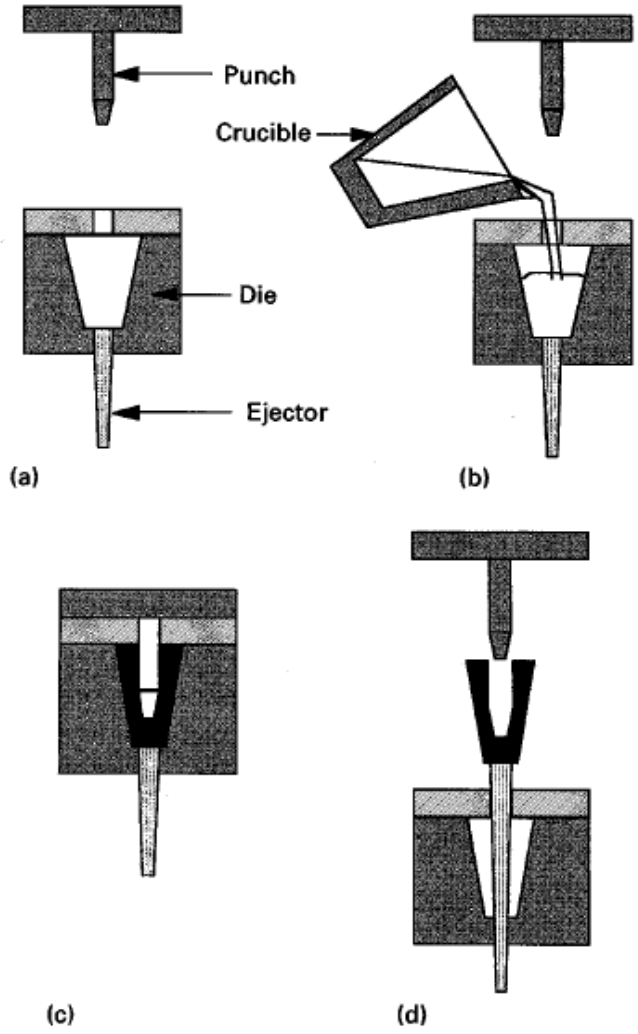

Figure 4: Squeeze casting process: a) die is preheated. b) metal melt transferred to die. c) solidification under pressure. d) ejection from die [15]

Because of its ability to eliminate porosity, squeeze casting is ideal for infiltration of a metal into a fiber preform. The fiber preform is made by coating the fibers with a binder, such as colloidal silica, that will enable fiber handling and stabilize the preform shape at high temperatures. Pressures used in squeeze casting can range from 0.5 MPa [16] to 100 MPa [17]. Pressure is usually maintained from 30s [18] to 90s [10].

For untreated fibers, mechanical properties for squeeze-cast composites are surprisingly consistent. Li and Chao, in their study on carbide formation, achieved 32% rule-of-mixtures values in their as-cast, low-carbide composite containing 12K PAN fibers [10]. This is similar to the strength values reported by Wang and Zhou [18]. The highest %ROM values reported, ~38%, are those of Bushby and Scott, who were using pitch-based fibers and an Al-5wt%Cu alloy [19].

One problem with squeeze casting is that it requires the development of expensive tooling. Aside from requiring a furnace and source of hydraulic pressure, squeeze casting dies and rams have the duty of sustaining a high stress for extended periods at high temperature. This will result in the tooling being quite heavy. Additionally, the tooling must be machined to tight tolerances to prevent any metal leakage.

2.2.2 Ultrasonic infiltration and gas pressure infiltration

In the development of broad, high-surface-area shapes like sheets and tubes, composite production is a two step process consisting of precursor filament production, and subsequent coalescence of those filaments into lamina in a hot-pressing procedure known as diffusion bonding. Precursor filament production is the most important stage in composite production, as it is the step in which the composite proper is created, albeit in small units. Secondary processing of precursor filaments through diffusion bonding does not require addressing nearly as many interfacial and wettability concerns. It is only available as an option after the true problems between aluminum and carbon have been addressed.

Precursor filaments are usually produced by ultrasonic infiltration. This process consists of immersing an ultrasonic horn into an aluminum melt, and then drawing fibers through the melt, either under or through the horn so as to receive a large amount of acoustic pressure. A schematic of the process is visible in Figure 5.

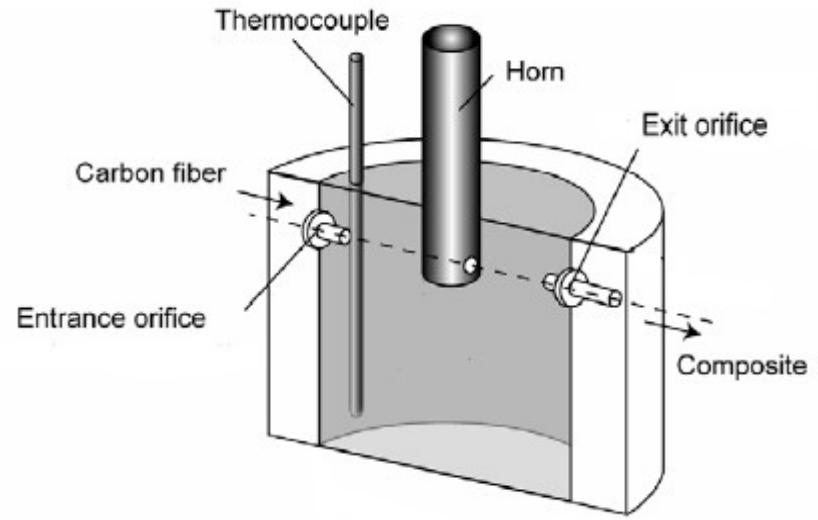

Figure 5: Schematic of ultrasonic infiltration process. [25]

Ultrasonic infiltration operates on the basis that sound causes an acoustic pressure that is proportional to both its frequency and amplitude. More precisely [20]:

$$p_m = \rho c \omega A$$

where p_m is the maximum acoustic pressure, ρ is the density of the medium, c is the propagation velocity in that medium, ω is the angular frequency, and A is the amplitude. Since ultrasound by nature consists of frequencies in excess of 20 kHz, and given that sound propagates an order of magnitude faster in aluminum compared to air [21], high

pressures are indeed achievable. Common stated operating acoustic pressures are in the range of several kilopascals up to 12.7 MPa [22]. However, high pressures are not necessarily required for composite production. It is known that for acoustic pressure amplitudes below a certain threshold, the phenomenon of cavitation will occur. Cheng et al. report this threshold to be less than 2 MPa [20].

In ideal conditions, cavitation occurs when small bubbles nucleate from a liquid as a result of pressure dropping below the vapor pressure of the liquid [23]. In essence, the liquid is locally displaced faster than other liquid can fill the void. This is sometimes described as exceeding the tensile strength of the liquid. Under practical conditions, cavitation generally occurs prior to pressure dropping below the liquid vapor pressure. This is because many liquids contain dissolved gases and impurities that act as nucleation sites. Bubbles formed at these sites possess a very low gas pressure, either as a result of nucleating directly from an existing gas bubble in the fiber tow or from the absorption of dissolved gases from the melt. Because the bubbles are surrounded by liquid of a higher pressure, they are compressed to the point of collapse. The collapse causes pressures within the bubble to reach upwards of several thousand atmospheres, and temperatures of several thousand kelvin [20]. This can be accompanied by shock waves and inrush of liquid traveling at speeds up to 400 m/s [24]. These effects serve to break any impeding particles, such as an inert oxide film, and encourage liquid flow within tight crevices.

Cavitation is one of the primary advantages of using ultrasonic infiltration, to the point that its occurrence is considered a criterion for infiltration [20]. It allows for low-risk, low-investment production of well-infiltrated composites. Matsunaga [25], in studying effect of magnesium content on PAN fiber/aluminum alloy composites, was

able to produce continuous lengths of precursor filaments possessing 70% ROM properties. His work was based on that of Cheng [20], who produced composites possessing 76% ROM values using PAN fibers and a pure aluminum matrix.

One issue that remains with ultrasonic infiltration is that impurities which ease the onset of cavitation may undermine the mechanical properties of the composite. The most common impurity is entrapped gases within a fiber tow. These are maintained in the microstructure of the composite as voids. Voids lower the area available for load bearing, inhibit load transfer between matrix and fiber and can serve as crack initiation sites. A SEM micrograph of a composite void is visible in Figure 6.

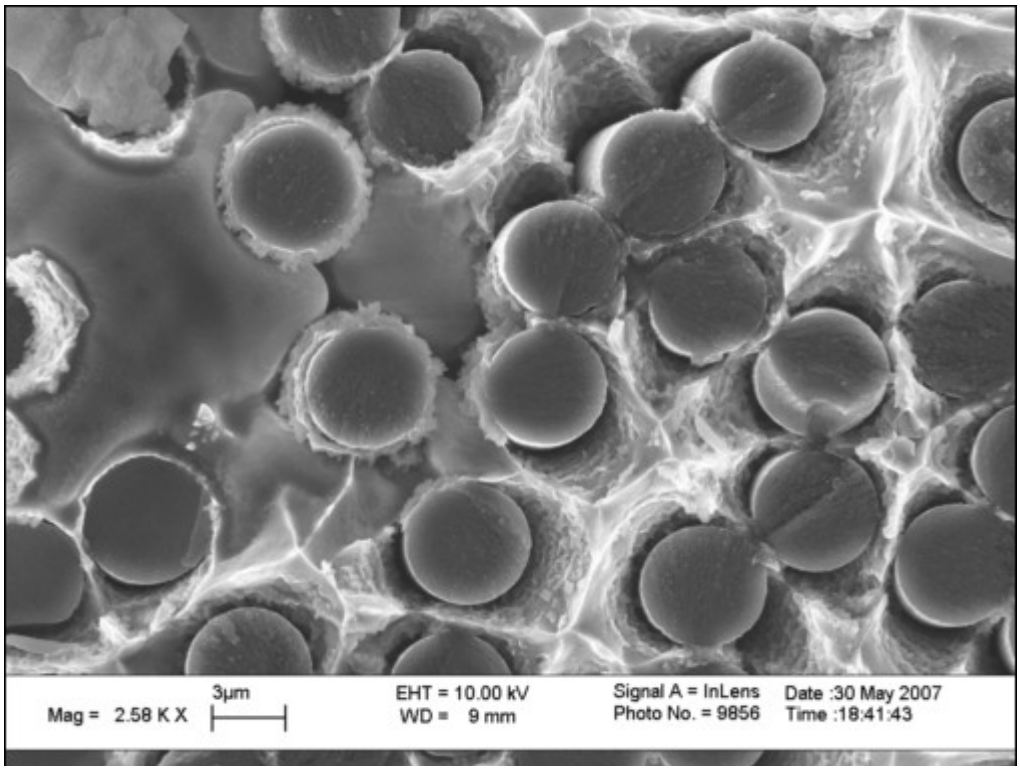

Figure 6: SEM micrograph of a composite sample broken in tension. Left portion displays a void region, marked by noncontiguous matrix region, and no evidence of plastic yielding as compared to matrix in the right portion of the micrograph.

2.2.3 Gas Pressure Infiltration

Gas pressure is often used in lieu of mechanical pressure in squeeze casting, or acoustic pressure in ultrasonic infiltration. For squeeze casting applications, gas pressure infiltration can allow for the production of different shapes without having to make drastic changes to the geometry of the die and the ram. The pressures used in those applications are similar to those employing mechanical pressure, but often the mechanical properties are improved. Plain fiber composites produced by traditional squeeze casting tend to have %ROM properties below 40%, whereas Friler [26] produced composites using pitch-based fibers in pure aluminum, and achieved 50% ROM properties. As well, Zhenhai [27] produced composites with plain PAN fibers, obtaining near 90% ROM properties.

The most notable device used for producing precursor filaments with gas pressure is that developed by Blucher [28]. It consists of a chamber with an aluminum melt at the bottom. The chamber is pressurized to 3.5 MPa with argon and has a hole at the bottom of the melt through which fibers are drawn upward. A schematic of the apparatus is visible in Figure 7.

Fibers are drawn at a very precise rate; because of gravity and the high pressure, aluminum will tend flow out of the bottom of the chamber. Fibers must be drawn through the entrance orifice at such a rate that all aluminum being forced out of the chamber by the gas pressure is subsequently frozen around the entering fiber tow and returned to the melt as infiltration proceeds.

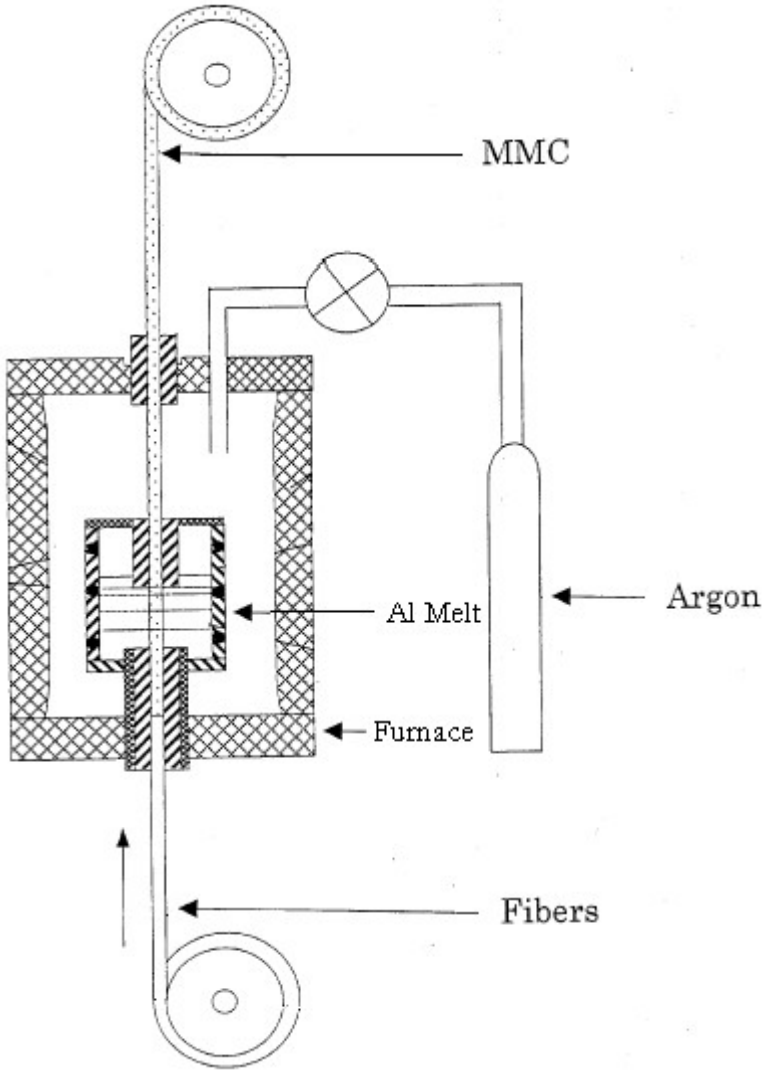

Figure 7: Precursor filament production using gas pressure infiltration. Fibers enter at the bottom of the pressurized chamber through the aluminum melt and exit at the top.

With this apparatus, Blucher claims [28] to produce composite precursor filaments possessing strengths far in excess of 100% ROM values – in some cases up to 150% ROM. He attributes this to the effect of high production speed: faster production speeds induce faster cooling rates in the matrix, giving a fine-grained microstructure. While the effect of microstructure on matrix strength is considered minimal, it is thought to play a significant role in improving load transfer between fiber and matrix.

Furthermore, faster production speed limits the exposure time between the fibers and molten metal, reducing carbide formation.

Because Blucher's results are some of the best reported concerning production of carbon fiber-reinforced aluminum, one would be tempted to reproduce his procedure as closely as possible. However, aside from intellectual property issues regarding Blucher's device in particular [29], gas pressure infiltration devices as a whole carry with them several risks and precautions.

Unlike solids and liquids, gases undergo significant reduction in volume with applied pressure. Any pressurized gas vessel is inherently a stored energy device, and explosion is always a risk. From a practical standpoint, vessels to contain a pressurized gas should be designed to withstand at least twice the pressure at which they will be operated. Legally, operation of a pressure vessel requires certification by OSHA. OSHA regulations [30] require that all pressure vessels be hydrostatically tested to 50% overpressure every year the vessel is in operation.

Depending on the volume of the pressure vessel, several precautions should be taken to reduce the damage caused in the event of an explosion. The vessel should be surrounded by sandbags to reduce shrapnel. For larger volumes, a blast wall might be appropriate as well, but is less likely to be necessary since the gases used for gas pressure infiltration tend to be argon or nitrogen and these gases do not present a combustion hazard. However, measures should be taken to ensure that the gas does not present a suffocation hazard.

2.2.4 Alloying Additions

Many of the alloying additions used in composite fabrication are for the purpose of improving infiltration behavior rather than increasing the strength of the matrix. These elements improve infiltration by lowering the surface tension of the aluminum and/or preventing uptake of an element by the aluminum. Some elements, such as lithium and magnesium, serve both roles equally well. This is perhaps the reason magnesium is the most common alloying element.

Small additions of magnesium (up to 10 wt%) are considered to aid in the wetting of carbon fibers by the aluminum. 10 weight % magnesium is considered an upper limit because Matsunaga [25] found that high magnesium content caused composites produced by ultrasound to possess below 50% ROM properties, where as they possessed close to 70% ROM properties with lower Mg content. He attributes this to a higher concentration of the hard and brittle Al_3Mg_2 intermetallic compound, similar to the effect of aluminum carbide on composite mechanical properties.

In describing how small Mg additions produce beneficial effects, Pai [31] proposes that many reinforcements possess about their surface a layer of adsorbed gases that inhibits intimate contact between matrix and reinforcement. Magnesium addition is able to thin this layer by oxygen uptake. Delannay [7] proposes that the magnesium substitutes for aluminum in its the oxide layer. This causes a weakening of the oxide layer. Although he does not elaborate upon the exact mechanism of this weakening, one can suppose it is a result of oxygen voids introduced in to the film as a result of coordination number differences between magnesium oxide and aluminum oxide.

Additionally, there may be some lattice mismatch between MgO and Al_2O_3, introducing incoherent interfaces where there previously had been none.

The second most common alloying element is silicon. Although silicon does not reduce the surface tension of aluminum, claims [32][33] have been made that it improves wettability by reacting with the carbon fiber to form silicon carbide. In this way, silicon shields active portions of the fiber surface from reacting with the aluminum. Because the silicon carbide-carbon fiber bond is stronger than the aluminum carbide-carbon fiber bond, wetting is improved. The contradictory evidence, presented in [32] as well, is that aluminum is a stronger carbide former than silicon at 800°C, proceeding via the following reaction:

$$3SiC(s) + 4Al(l) \rightarrow 3Si(l) + Al_4C_3(s)$$

Composites containing SiC coatings on carbon fibers occasionally feature [34] a matrix with a high silicon content. The purpose of this is to suppress the Al/SiC reaction, according to LeChatelier's principle.

Like magnesium, silicon content is usually limited to around 12 wt% maxiumum [35], as Al-Si alloys compose the 4xxx series of aluminum alloys, known for their low thermal expansion at the expense of toughness. Etter [36] noted the formation of Mg_2Si particles in an carbon fiber-aluminum alloy composite that was thermally cycled. These particles seemed to serve a similar detrimental purpose as the Al_3Mg_2 particles mentioned previously.

2.2.5 Fiber Coatings

By far the most common method of improving composite properties has been through the use of fiber coatings. When research into fabrication techniques of carbon fiber/aluminum composites was first conducted in the 1970s, carbon fiber's full utility as a reinforcement material was severely limited by its high cost, which is no longer an issue. At that time, these composites were considered exotic, high-technology materials, such that little emphasis was placed on researching practical, economic means of manufacture, inclusive of the fiber coating procedure. What emerged from such early research was a coating composed of titanium diboride, reported by Harrigan and Flowers [37] in 1976. Titanium diboride is a hard corrosion- and wear-resistant material, applied by chemical or physical vapor deposition. Composites manufactured from these fibers displayed good wetting and no harmful interfacial reaction product, but successful adaptation of this coating was hindered by its cost, shadowing effects inherent to the deposition process, and the instability of the coatings in air.

In the time since, coating research has progressed towards solutions that are less expensive and easier to apply. Most coatings are applied through a solution bath of some sort, such as electroless deposition or sol-gel. More common materials are used, such as metal oxides or first period transition metals. Typically, metallic coatings are applied to address wetting concerns, while ceramic coatings are applied to act as a diffusion barrier, although coatings can often serve both purposes.

2.2.5.1 Metallic coatings

The wetting improvement seen with the metallic coatings is attributable to the fact that liquid metals will very often wet solid metals, even if the metals have low mutual solubility [7]. Because of this, a large variety of metals have been tested as fiber coatings: chromium, nickel, copper, gold, molybdenum, cobalt, silver, lead, thallium, titanium, tantalum and more have all been candidates as fiber coatings. Several reasons, from toxicity (chromium, thallium) to cost (gold, tantalum, molybdenum, silver) have eliminated many of these metals as viable fiber coatings. The two remaining popular coatings for carbon fibers are nickel and copper.

Many sources [38][39][7] recognize the formation of intermetallic compounds as being central to the wetting improvement of the Ni and Cu coatings. These compounds are typically Al_3Ni, Ni_3Al_2 or $CuAl_2$. The mechanism of wetting is still unknown, however. Some claim that the formation of intermetallic compounds creates a strong bond across the fiber/matrix interface [38], while others consider the intermetallics as a byproduct of coating dissolution that allows for the aluminum to contact a "fresh" surface of the carbon fiber [40].

Both types of coatings are applied by electroless deposition. At one point cementation was also a popular method of producing coatings, but it produces a coating with more defects. This has the effect of reducing the strength of the coated fiber [39], but no damage occurs to the fiber proper. Each method can be used to produce a coating of thickness one micron or less, so as to minimize free intermetallic precipitates in the matrix. These can cause brittleness, much like other intermetallic compounds already

discussed. Additionally, a copper or nickel coating of 1 μm on 7 μm fibers will contribute ~5 at% Cu or Ni to the composite, at only 5% fiber volume fraction.

Electroless deposition is a common procedure for metal plating, but cementation is perhaps not as well known. In cementation, a metal is precipitated from a salt solution through the introduction of a more active metal. A cementation reaction for producing a nickel coating is:

$$Ni^{+2}SO_4^{-2} + Mg^0 \rightarrow Mg^{+2}SO_4^{-2} + Ni^0$$

although another salt such as $NiCl_2$ could be used as well. Carbon fibers are treated with glacial acetic acid prior to immersion in the salt solution so as to tag their surfaces with polar carboxyl groups. The negative dipole of the carboxyl group attracts Ni ions, which become ionized shortly after being displaced from the salt [40].

One aspect that remains unclear is the purity of coatings created by the cementation process. Although research that uses the cementation technique claims to produce pure nickel coatings without providing elemental analysis details, one would think that even though the dissociation constant for magnesium sulfate is lower than for nickel sulfate, some dissociation would still occur, and the coatings would possess some amount of magnesium content.

Unfortunately, there are no reported mechanical properties of composites produced with Ni or Cu coatings, as much of the research employing these coatings is concerned only with composite manufacture and interfacial interactions. However, even though composite manufacture is very often successful, many groups that report on the usage of metallic coatings fabricate composites with pressure assistance [16][41][17] or

with chopped fibers [42] that do not have as many infiltration problems. These methods cast doubt to the effectiveness of the coatings as wetting agents. Furthermore, their effectiveness as diffusion barriers is unclear: some groups report that copper intermetallics, unlike the nickel intermetallics, dissolve completely in the matrix and are therefore not present to aid in bonding the fiber within the matrix or protecting it [42]. Other groups report the opposite, claiming that nickel coatings dissolve into the matrix [43]. Of particular note is the work of Wielage and Dorner [44], who observed that nickel coatings were extremely susceptible to electrochemical corrosion attack as a result of the nickel forming intermetallic compounds and being removed from the fiber. The newly formed intermetallics can act as cathodic sites just as the fibers do, increasing the corrosion current density.

2.2.5.2 Fluoride salts

A special class of fiber coatings is those composed of fluoride salts. These salts are commonly used fluxes in processing aluminum melts because metal oxides display a slight solubility in certain alkali fluoride salts, such as K_2ZrF_6, K_2TiF_6, and Na_2SiF_6 [45]. Such salts find use in composite processing as aqueous solutions that can be used as a fiber coating to dissolve any aluminum oxide film impeding interaction. K_2ZrF_6 is the most commonly used salt because it is the most soluble in water as compared to K_2TaF_7 or K_2TiF_6.

As can be seen in Figure 8, wetting angle between carbon and aluminum decreases significantly with fluoride treatment. Presumably, this is the result of both the

aluminum oxide film being removed and the formation of carbide at the fiber/bare metal interface. Hence, these coatings are best utilized atop more protective fiber coatings as they can cause significant damage to the bare fiber [46]. Although the mechanism of fiber damage is nowhere referred to as being the result of carbide formation, extent of degradation is directly related to contact time between fiber and molten aluminum, visible in Figure 9.

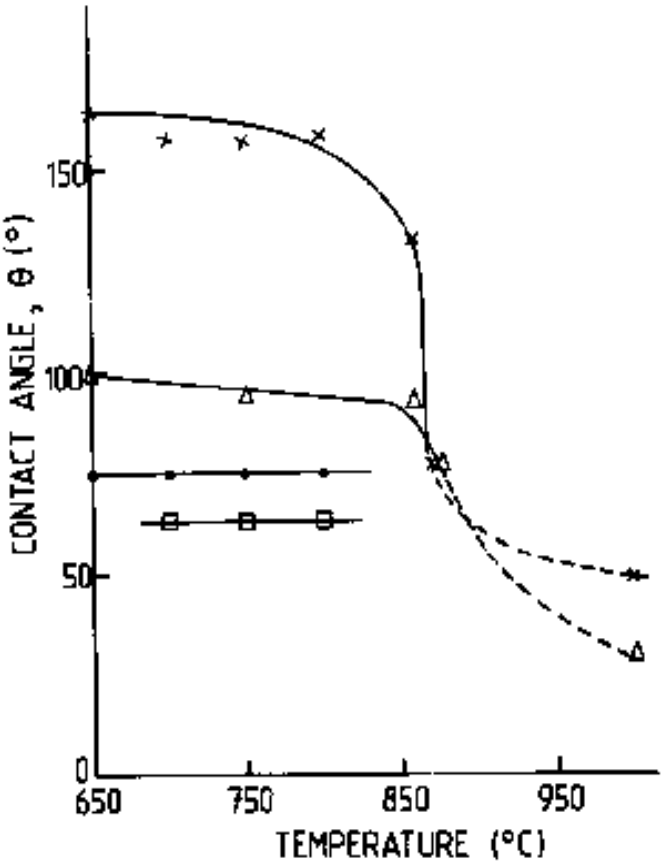

Figure 8: Variation of contact angle with temperature for a sessile drop of aluminum on a pyrolytic carbon substrate. x) no fluoride treatment; Δ) "slight" K_2ZrF_6 treatment; ●) 5 mg/cm^2 K_2ZrF_6 ; □) 12 mg/cm^2 K2ZrF6. [8].

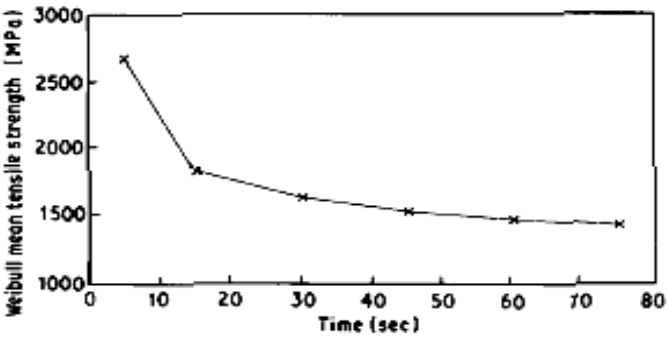

Figure 9: Variation of mean tensile strength of extracted carbon fibers with molten aluminum contact time. Temperature of the aluminum was 650°C [46].

2.2.5.3 Ceramic coatings

Ceramic coatings have traditionally been used as diffusion barriers. Ceramics are preferable to many metallic coatings because of their low density and use as reinforcing phases. Their downside is that they are brittle, and may require high temperature or exotic synthesis methods. Aside from the initial work with titanium boride, the ceramic coatings developed since that time have been primarily carbides and oxides. Carbides are chosen as fiber coatings because they are by nature an intermediate between carbon and metal, which should be ideal for a carbon/metal interface. Their drawbacks are that many carbides have to be produced by vapor deposition, and that all carbides are electrically conductive, thus providing no corrosion protection. Oxide coatings are used because they can be more easily synthesized and wetting might result through oxide reduction by the aluminum. They may not be as adherent to the fiber surface, however.

The two most common carbide coatings are silicon carbide and titanium carbide. Silicon carbide has received the most attention, probably as a result of it being a well-

studied material and finding use on its own as a reinforcing phase for metal matrix composites. Silicon carbide is usually applied via a vapor deposition process [34] or through pyrolysis of a polycarbosilane polymer [18]. Because it is a carbide, it is more adherent to the fiber surface than a metal coating, and is used as a barrier between a fluoride salt wetting treatment and the bare fiber [34][8] to prevent the bare fiber from reacting with the aluminum metal. As mentioned earlier, silicon carbide is a less stable carbide than aluminum carbide. In these applications, silicon carbide seems to serve the purpose of a sacrificial coating, where the detrimental effect of carbon fiber/aluminum contact is interpreted as the loss of high strength fiber rather than gain of brittle, hygroscopic carbide. The degradation is then controlled with large cooling rates and/or the use of an Al-Si matrix to prevent complete dissolution of the SiC coating in to the matrix.

Mechanical properties data are somewhat unclear regarding the efficacy of fiber coatings in improving the strength of composites. Friler [26] used a CVD-applied layer of SiC on pitch-based carbon fibers. They were infiltrated in to aluminum under a gas pressure of 55 atm (5.5 MPa). With this method, he obtained %ROM strengths of near 74%. It should be noted that this is in contrast to %ROM strength of 65% using uncoated fibers.

Wang [18] obtained respectable strengths of 675 MPa in composites using polycarbosilane-derived SiC coatings on PAN fibers, but the range of the fiber strength, the volume fraction, and the applied pressure (10-60MPa) make it difficult to draw conclusions about his fabrication processes. A strength of 675MPa could be as high as

75%ROM or as low as 42%ROM. 42%ROM is not altogether mediocre for this class of composites, unless it required 60 MPa to produce it.

Titanium carbide coatings were briefly studied because they are theoretically more stable than aluminum carbide and should not be degraded by contact with the metal [47]. Perhaps the main reason titanium carbide was studied was the fact that a method emerged that allowed for a TiC conversion coating to be produced using a low-temperature Sn-Ti bath. This method, called liquid metal transfer agent, provided a very attractive alternative to CVD, the traditional method for TiC coating.

Liquid metal transfer agent involves the use of a molten metal bath that contains a small addition of a carbide forming element, such as 1 wt% titanium. Tin is used as the bath metal because of its relatively low melting point and unwetting behavior towards graphite. Carbon fibers are dipped in the bath, where the titanium reacts with their surface to form a titanium carbide "conversion coating," since the outer surface of the fiber has undergone a reaction to produce the coating. Excess tin is then dissolved with HCl or within the aluminum matrix.

Himbeault et al. [48] are the only group to report mechanical properties of composites produced with titanium carbide-coated fibers. The properties of the resultant composites are excellent: several reported cases of near 100% ROM strengths for both an Al-10%Mg and Al-12%Si matrix. The fact that such good properties were obtained is even more notable because not only does the coating slightly degrade the fibers, but also the composites were produced simply by dipping the carbon fiber/TiC/Sn ingot in to an aluminum melt.

Oxide coatings are the final class of popular ceramic coatings. The oxides used as fiber coatings are common ones, with alumina, silica, zirconia, and titania being prevalent. Like the carbides and the metals, an oxide coating is chosen largely because of the class of materials to which it belongs. Much of the appeal of an oxide coating stems from its ease of manufacture through the sol-gel process.

The sol-gel process involves the formation of a colloidal network of hydrated metal ions through the hydrolysis in a solution of metal alkoxides or metal salts [49]. Alkoxide hydrolysis is accomplished with the use of an alcohol solution, while water is typically used for salt hydrolysis. The network is then pyrolyzed to produce the desired oxide. The process allows for low temperature, precise synthesis of metal oxides. Unlike traditional ceramic mixing techniques, the oxide precursors are mixed on an atomic level, allowing for the synthesis of homogeneous multicomponent oxides. As well, since the oxide is derived from a solution, sol-gel is ideal for fabricating thin films and complex shapes.

Oxide coatings have been shown to cause some improvement in mechanical properties of composites. The best reported results are those of Katzman [50], who studied silica coatings and claims to have produced composite samples possessing 80% - 95% rule of mixtures strengths. Peng et al. [51] achieved ROM tensile strength of 35% using an aluminum oxide/amorphous carbon dual coating, as compared to a ROM tensile strength of 25% with the plain fiber. As well, Zeng [52] achieved 48% ROM tensile strength using an aluminum oxide coating with ultrasonic infiltration. However, this is in comparison to a 42% ROM strength with plain fibers. He noticed markedly improved infiltration on coated fibers, as samples produced with uncoated fibers contained a void at

their center, as if the metal melt could not penetrate that deeply. This is similar to the results of Clement [53], who studied titanium dioxide coatings and found them to improve wetting in an aluminum matrix through oxide reduction. This oxide in particular is not the best choice for improving the wettability, as the anatase to rutile phase transformation occurs in titanium dioxide at temperatures near the aluminum melt temperature, and it has a disruptively large volume change associated with it.

3. OBJECTIVES

Several different approaches are clearly possible in producing composites with good mechanical properties. One could take a manufacturing-based approach and simply optimize that process to minimize fiber/metal contact time, cover interfaces from environmental exposure, treat the fibers to reduce entrapped gases, etc. However, in light of so many potential interfacial problems between the fibers and the aluminum, it seems circumspect to apply a chemistry-based approach as well and develop a fiber coating. Many processes do exist for producing low-cost coatings, so such an approach is not out of the scope of the project. As well, since this research concerns the development of a continuous manufacturing process, should some parameter in that process become altered, it could result in poor quality across some length of that composite. By nature of being a continuous process, presumably one would want composites that are of substantial length and not interrupted by removal of low-quality regions.

3.1 Develop a fiber coating

The primary objective of this project then is to develop a fiber coating that is inexpensive, makes minimal use of harmful chemicals, and is adaptable to an in-line manufacturing process. From these criteria, several candidates for coating materials and coating processes can be eliminated.

Of the possible coating materials, precious metals and those derived from hazardous solutions, such as chromic acid used in electroplating of chromium, are not candidates. Fluoride-based wetting agents are also not an option – many, if not all, ionically-bonded fluoride compounds are extremely reactive and hence, toxic. Their use and disposal are subject to strict environmental regulations [54].

Vapor deposition is not an option because of its large initial capital investment and the continued cost of an inefficient process. In vapor deposition the entire reaction chamber is coated, so only a small portion of the precursor materials contribute to the formation of a fiber coating. As well, a large amount of the precursors remain unreacted. The precursors often used in vapor deposition are metal chlorides, such as $TiCl_4$ and BCl_3 for the titanium boride coating. These compounds are corrosive as-is, and their reaction produces hydrochloric acid [55]. These products and byproducts are even more of a nuisance because they exist as a vapor and need to be scrubbed or condensed to be dealt with appropriately.

The ideal coating process is thus one that makes use of a solution coating process, with slight preference given to aqueous processes for minimizing the use of organic chemicals. These allow for efficient use of precursors, in-line adaptability, and efficient collection of byproducts. Since these processes tend to use metal salts or a tin solution, their cost should be reasonable.

3.2 Develop manufacturing technique

The secondary objective of this research is first to develop both a small-scale method of producing samples to evaluate fiber coatings in their interactions with the fiber and matrix. Second, in-line fabrication of composite samples will be conducted. The only true candidate for in-line fabrication is ultrasonic infiltration, while either squeeze casting or gas pressure infiltration are probably the best choice for small sample production.

4. RESULTS

The fiber coatings used in this study are zirconia, also known as zirconium oxide, or ZrO_2, and alumina, also known as aluminum oxide or Al_2O_3. These coatings were applied to Hexcel IM7 PAN carbon fibers, in 12K tows, and to some extent on Toho G30 PAN fibers in 3K tows. The IM7 fibers were studied much more extensively than the G30 fibers, as the G30 fibers were already coated in a polymer sizing. This sizing is for the purposes of improving adhesion and infiltration behavior of the fibers in a polymer matrix, but it only adds an additional processing step for metal matrix applications. It was found that the sizing could be burned off of the fibers (Figure 10), but there was no compelling reason to study coatings on one fiber versus the other.

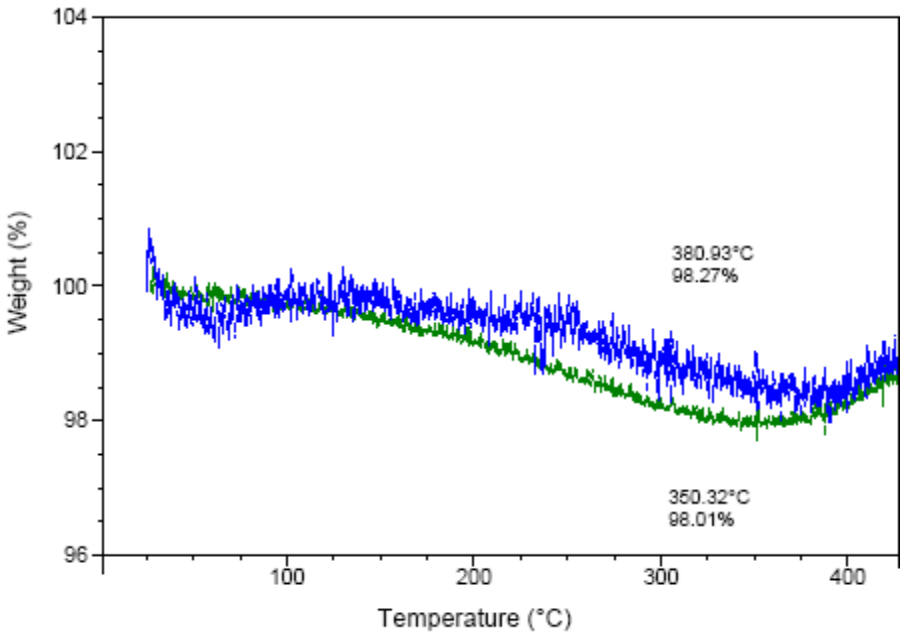

Figure 10: TGA trace revealing weight loss of sized fibers near 380°C.

4.1 Zirconia coating

The ZrO_2-based coating is the first coating that was produced. In addition to the aforementioned benefits of a nonconductive coating, the zirconia coating in particular was chosen for its ease of application and the low cost of its precursor materials. There also exists the possibility of wetting improvement through oxide reduction by the aluminum metal. A zirconia coating could act as a stress gradient to relieve some of the compressive hoop stresses about the carbon fiber. The coefficient of thermal expansion of zirconia is approximately 8 ppm/°K, in between those of aluminum and carbon.

The method for producing the coating was adopted from the work of Geiculescu et al [56]. It is an aqueous sol-gel based coating consisting of dip-coating carbon fibers in a solution of zirconium acetate in acetic acid containing 15% zirconium (Aldrich). Because Geiculescu developed her process specifically for coating carbon fibers, the procedure is carried out unmodified for our application: fibers are dipped for 1 minute in a 2.5 vol. % solution of the zirconium acetate in distilled water. The coated fibers are dried at 60ºC for 30 minutes and pyrolyzed at either 555ºC or 745ºC for an additional 30 minutes. TGA analysis shows that plain carbon fibers oxidize readily at 500 ºC, so both heat treatments were conducted in an Ar or N_2 environment.

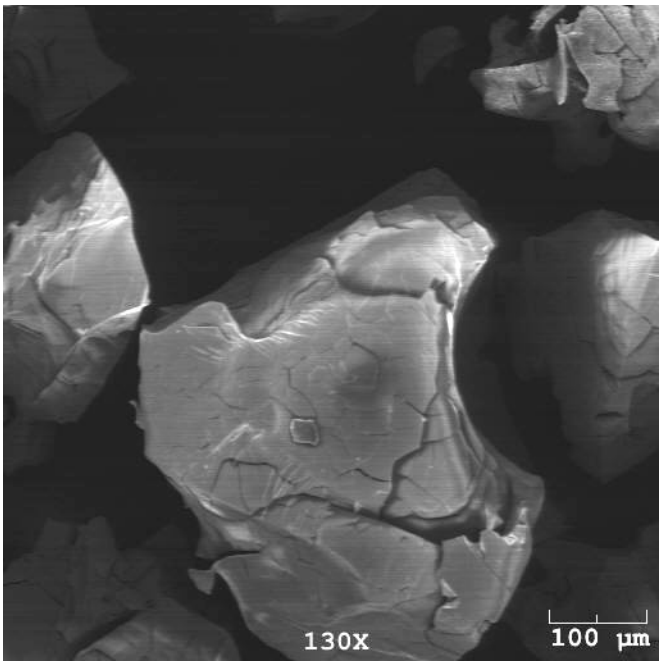

Figure 11: Zirconia crystals produced from drying and firing zirconium acetate solution

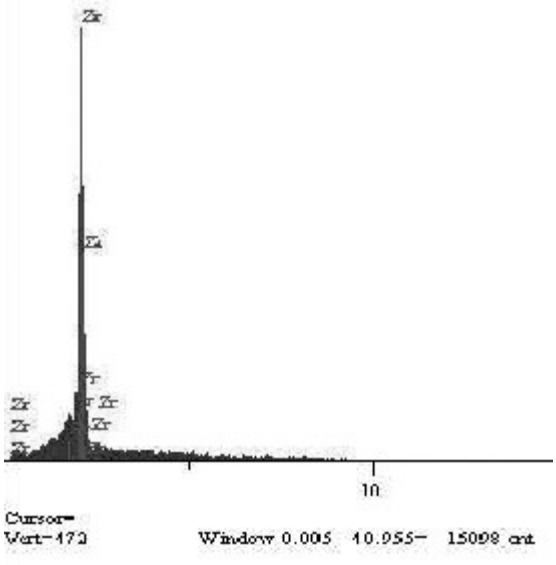

Figure 12: Presence of zirconium as confirmed by the Hitachi S-800 EDX detector. Detector can detect elements as light as fluorine.

The quality of coating produced by this method was unknown for some time, as any coating that was produced was also quite delicate. Coating presence was analyzed using a Hitachi S-800 SEM. In the course of mounting fiber samples on an SEM sample stage, it was common practice to spread the fiber tow out on the stage so that as many fibers as possible could be viewed. This would damage the coating on the outer fibers and leave many of the inner fibers in pristine condition. However, it was unknown if the pristine fibers were simply undamaged from sample mounting or if the dip-coating solution had failed to penetrate within the crevices of the fiber tow. The easiest way to determine presence of a fiber coating was from the contrast present where the coating had cracked or separated from the fiber. The remaining fibers lack the contrast necessary to determine if they were perfectly coated or perfectly uncoated. EDX analysis would confirm or discount the presence of zirconium, but the meaning of that result was often unclear, as it was unknown over what portion of the sample the data were obtained, and high-count x-ray signals were only obtained at lower magnifications.

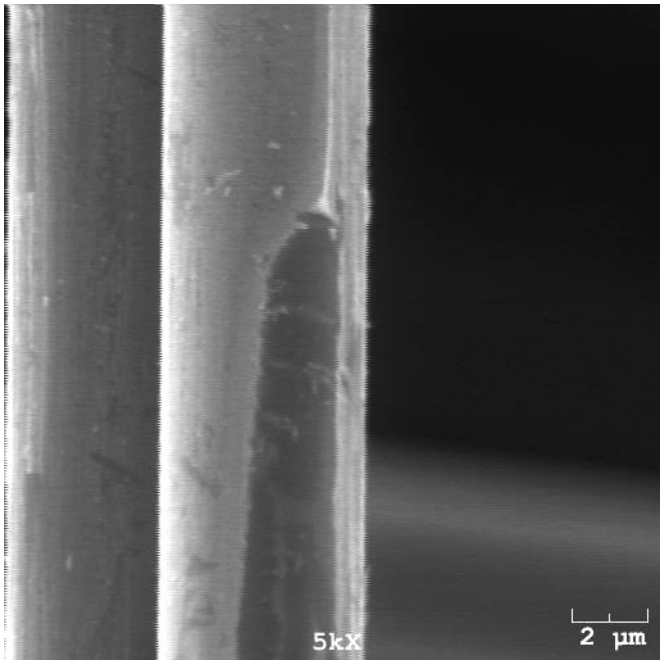

Figure 13: Cracked zirconia coating from 2.5% solution on IM7 fiber. Underlying fiber is visible as the darker region.

The ambiguous results of the coating method led to experimenting with several parameters, such as longer dip times, different pyrolyzing schedules, different forms of agitating the fibers during dipping, and different solution concentrations. Many of the samples produced from these iterations appeared similar to others – damaged fibers and many perfect fibers. During viewing of a sample that had been dipped for 2 minutes and pyrolyzed at 745ºC, a particular fiber was visible that had been evenly coated along only a portion of its length. The transition from defect-free coating to damaged coating was plainly visible and it provided some clear evidence that the perfect-looking fibers were well coated.

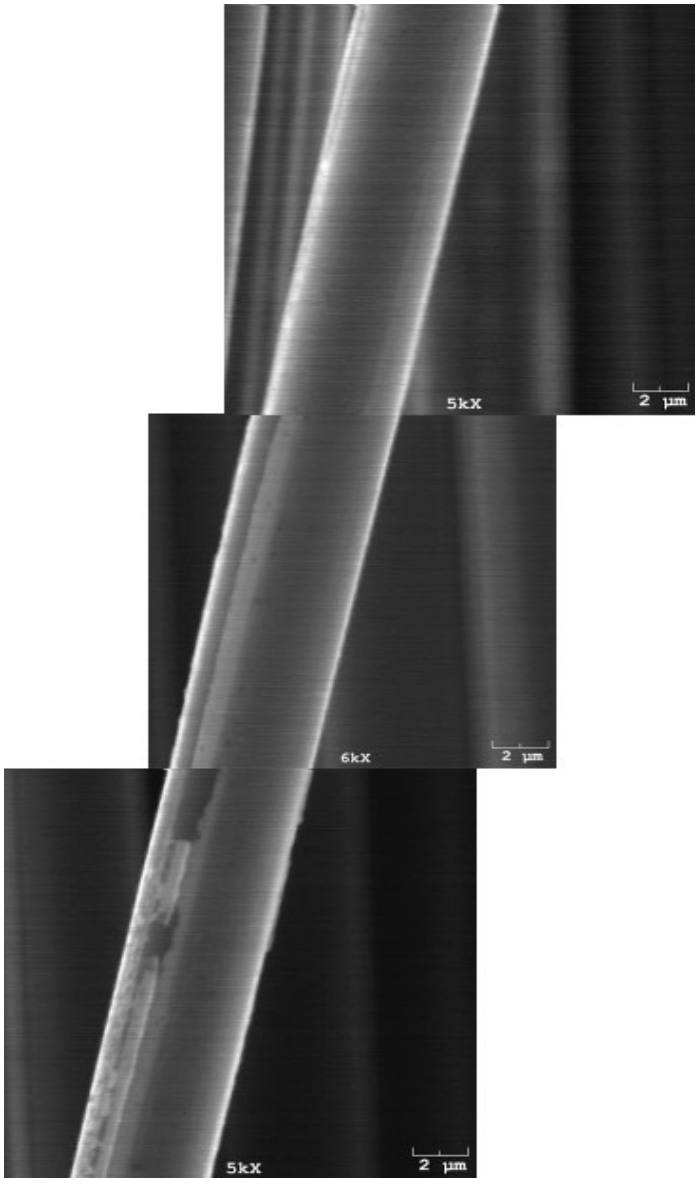

Figure 14: Top-down transition from "ambiguously perfect" to cracked coating, from 2.5% solution

4.2 Alumina coating

Aluminum oxide coatings were also studied, for many of the same reasons as the zirconia coating: the precursor materials are not expensive, and the method easily lends itself to a production line environment. Aluminum oxide has a thermal expansion of

approximately 8 ppm/ºK and could also act to relieve some compressive stresses about the fiber. It is unknown if the metal will reduce its own oxide, but this coating was pursued more as a protective barrier rather than a wetting agent. The coating was also realized through an aqueous sol-gel process, as originally described in work by Macêdo, Osawa and Bertran [57], as well as the work of Li and Pan [58].

The method of Macêdo et al requires dissolved aluminum nitrate salts (Aldrich) in distilled water up to the point of solution saturation (approximately 70g $Al(NO_3)_3$ per 100mL H_2O). Urea (Aldrich) is added such that the ratio of Al^{+3}/urea is 1/13 (approximately 152g urea per 100 mL H_2O). The solution can then be heated at 90ºC at 12h to form a viscous translucent gel, which is then dried at 300ºC for 25 minutes to form amorphous γ-Al_2O_3.

Because this process was developed for the production of aluminum oxide powder, some alterations had to be made to achieve an appropriate fiber coating. Many of the steps requiring long time excursions, such as the gelation and drying steps, could be eliminated or shorted significantly. Coating solution concentrations could likewise be reduced. Fibers dip-coated with the original concentration of sol form many millimeter-sized white precipitates on their surface after heat-treatment, and many precipitates and fiber bridges are visible even at solution dilutions of 100x. Dilution of 125x produces a uniform, bridge-free coating of about 100 nm in thickness.

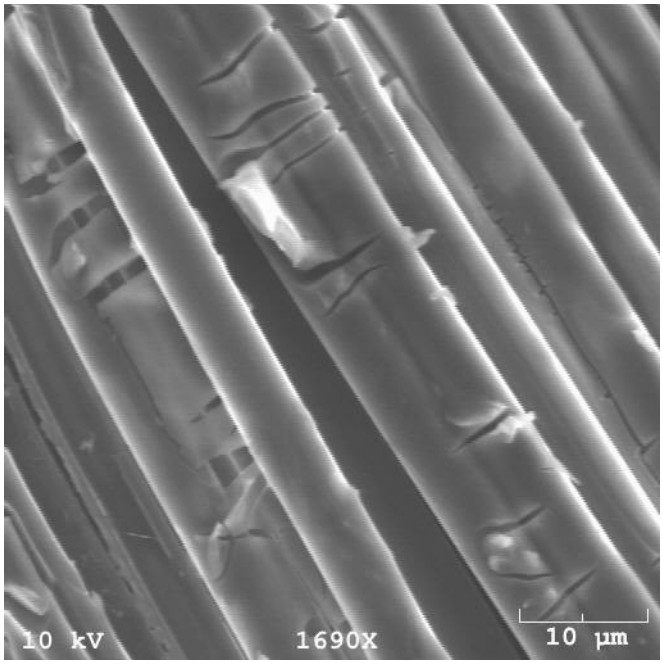

Figure 15: 1:100 dilution of original aluminum oxide solution. Fiber bridging and precipitates still evident.

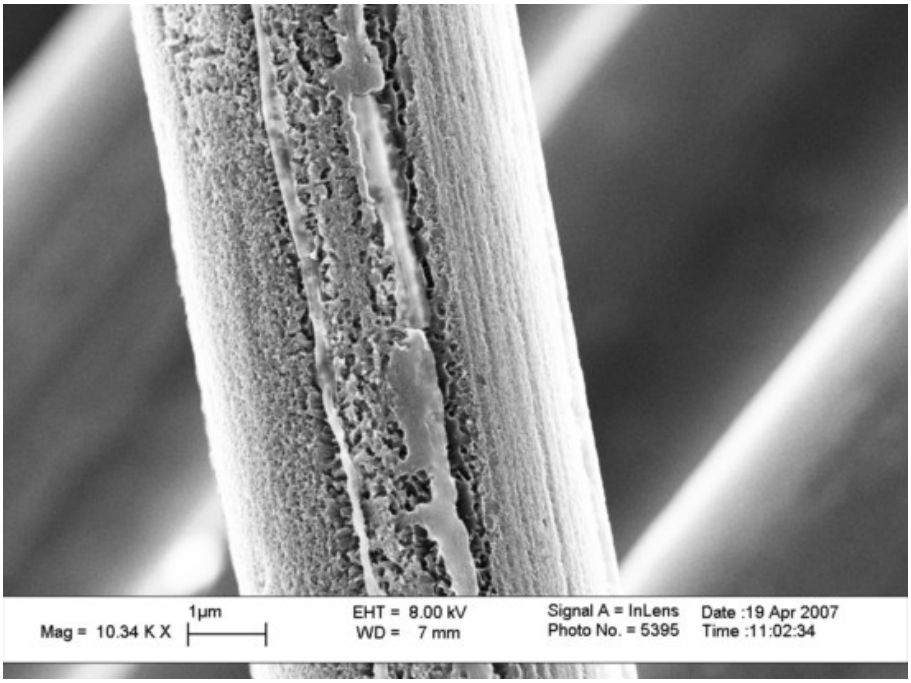

Figure 16: 1:125 dilution of the original aluminum oxide solution. Fiber is almost perfectly coated

Li and Pan's method also uses aluminum nitrate salts dissolved in water, but with the addition of citric acid (Aldrich) in place of urea. Aluminum nitrate is added to form a 0.5M solution, and citric acid is added to form a citrate/nitrate ratio of 0.5, 1, or 2. The solution is stirred at 60ºC until a yellow sol forms. It is heated to 200ºC to form a polymeric precursor, and calcined for 2 hours at various temperatures depending on the desired phase of aluminum oxide. This method was not pursued as a possible coating, as did not produce any discernible product, even at citrate/nitrate ratios of 0.5, 1, and 2. Only after approximately 6 months did solutions of citric acid and aluminum nitrate began to take on a yellow hue. Furthermore, the temperatures used in this method exceed those of the Macêdo method by at least 300ºC.

4.3 Composite Fabrication

Most documented aluminum-carbon fiber composite production techniques are complex and expensive, as it is difficult to apply pressure at high temperatures safely and effectively. Since the complex and expensive route was always an option, albeit an undesirable one, composite fabrication approaches were initially very simple, and became increasingly more complex as fewer alternatives remained. It should be noted that other research has been very clear that several of the fabrication methods employed in this project are not viable methods of composite production, per the previously mentioned wetting incompatibilities. Rather, these methods were used only to develop an understanding of the fiber-matrix interface at minimal expense and time.

4.3.1 Fiber "Sandwiches"

Early fabrication experiments focused on creating carbon fiber "sandwiches," with layers of fibers between thin aluminum sheets. The entity was expected to coalesce upon heating of the sandwich and melting of the aluminum, but this result was never achieved. Because of the ever-present aluminum oxide layer on its surface, molten aluminum slumps under its own weight, but does not readily mix or leak from its oxide container unless disturbed.

Attempts were made at reducing the effects of the oxide layer by etching the aluminum with a 25% w/v solution of NaOH in water. Even when the experiment was performed under nitrogen or argon atmosphere, fiber sandwiches often emerged from the furnace in only a distorted form of their original version, but still composed of distinct entities.

Figure 17: Fiber sandwich after emerging from the furnace; two aluminum sheets remain separate.

4.3.2 Fiber Dipping and Drawing

To circumvent the tenacity of the oxide layer, the approach of directly dipping fibers in to the aluminum melt was taken. With a pure melt, the fibers proved too fragile to penetrate the surface oxide layer, and this experiment was unsuccessful. In some experiments, an equimolar mixture of KCl and NaCl was used as a cover flux, as it melts at a temperature slightly below the melt temperature of aluminum [45] and will cover the surface to reduce oxidation. In this scenario, the fibers still had difficulty penetrating the aluminum surface, and wicked up a large amount of the liquid salt.

Finally, as a means of bypassing the surface oxide altogether, fibers were threaded through a hole at the end of a graphite rod. The rod was then immersed in an aluminum melt, and the fibers were manually drawn through the hole in the rod. They emerged from the melt with a thin layer of poorly adhered aluminum on the outer surface of the tow, and no infiltration to the inner filaments of the fiber tow. The effect is visible in Figure 18.

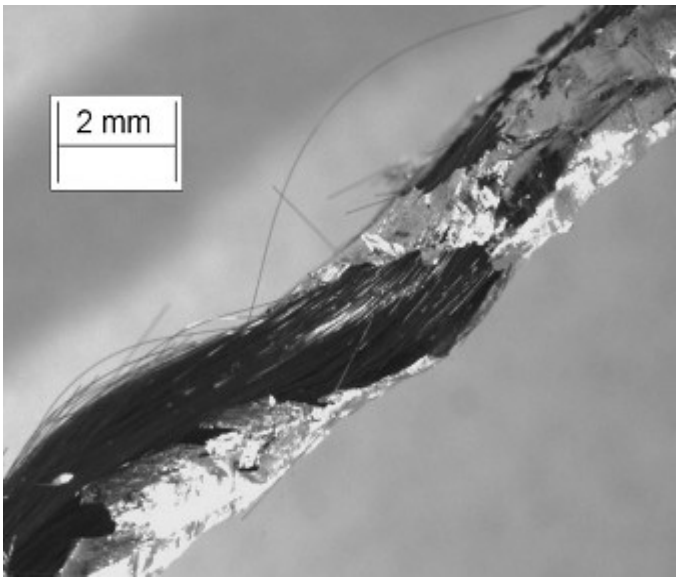

Figure 18: IM7 Fibers with poorly-adhered aluminum layer. No infiltration.

Because drawing was performed by hand, the effect of temperature difference between the fibers and the aluminum cannot be completely discounted. If the fibers were at any temperature significantly lower than the melt temperature of aluminum, then their insertion in to the melt would cause a thin aluminum shell to freeze around the tow. It is unknown what time is necessary for equilibration and re-melting of the aluminum shell, as well as whether the drawing speeds were slow enough to allow for re-melting. Because

this experiment was performed at a separate facility, it was difficult to repeat with pre-heated fibers or a slower drawing time.

4.3.3 Squeeze-Casting of Composite Samples

At this point, our research focused on developing pressure-assisted fabrication methods. At Georgia Tech, squeeze casting of small composite samples was pursued, while ultrasonic infiltration was simultaneously pursued at a separate facility.

An improvised squeeze casting apparatus was developed with two aluminum oxide rods and an aluminum oxide tube. The inside diameter of the tube nominally matched the outside diameter of the rods. An aluminum/fiber mixture was placed in the tube, and the rods were inserted in to opposite ends of the tube so that each butted up against the aluminum/fiber mixture. Manual pressure could be applied to the mixture by pushing the two rods together. The entire apparatus was inserted in to a mullite tube furnace, such that the ends of the rods extended out of the furnace tube, and pressure could be applied while the aluminum/fiber mixture was at temperature in the center of the furnace.

In two samples produced by this method, leaking occurred and fibers within the pellet remained a separate phase (Figure 19). The mere existence of even these poorly produced samples was a fortuitous event: because of a lag time between heating element temperature and actual furnace temperature, these two samples happened to be consolidated at a very soft/slightly molten temperature that limited leaking, and attempts at producing samples at any higher temperature resulted in complete leaking.

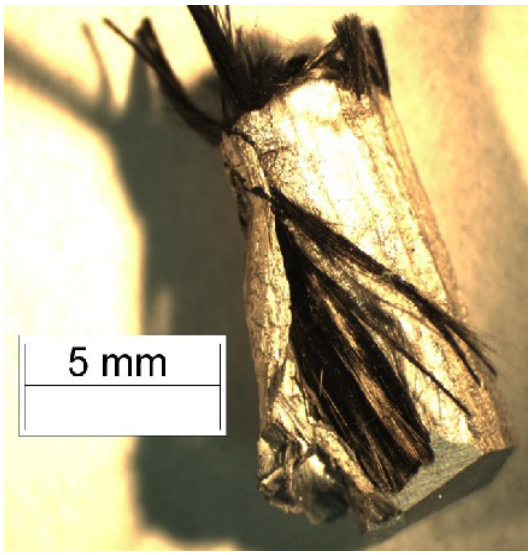

Figure 19: Pellet produced by applying pressure between aluminum oxide tubes. No infiltration

A stainless steel fixture was fabricated, consisting of a threaded plunger and a cup with removable bottom. It was machined at the Georgia Tech School of Mechanical Engineering machine shop to tolerances of ± 0.0005" in order to address the leaking problems present in the other fixture. Like the previous method with the aluminum oxide tube, a fiber and metal mixture would be packed in to the cup, and the plunger would be used to apply pressure to the mixture. The plunger threaded to an adapter attached to a fatigue-testing machine so that high and precise loads could be maintained. The entire fixture was contained within a furnace for melting the aluminum. The experiment was conducted with argon gas flowing through the furnace to minimize oxidation of the fibers, but gas-tight seals were not in place to make a truly oxygen-free environment. Surfaces in contact with the aluminum were coated with a boron nitride release agent (GE).

Figure 20: Stainless steel squeeze casting fixture: long threaded plunger and a cup with removable plug.

A fundamental problem with this approach, and all approaches requiring mechanical pressure, is that the tolerances of the pieces of the apparatus will almost certainly be much larger than the spaces between filaments within the fiber tow, and leaking will naturally occur at these larger gaps.

Experiments with this squeeze-casting fixture did leak extensively (Figure 21), at times requiring up to 8,000 pounds of force to separate the seized pieces of the fixture. It was anticipated that the boron nitride release agent would act to seal some of the gaps in the fixture, but alternative sealing materials were pursued as this proved not to be the case. Cup-shaped gaskets were used to contain the fiber-metal mixture. They were made from Grafoil graphite sheet or from flared copper cups that were press-fit in to the fixture.

Neither was successful in preventing complete metal leakage. In several cases the copper cups would dissolve in to the molten aluminum.

Figure 21: Leaking of metal from the squeeze casting fixture

Although metal leaked from this fixture in each experiment performed, a small pellet of metal would remain in the fixture after leaking had subsided under the applied load. However, even with applied pressures of up to 775 psi, the remaining metal pellet displayed little fiber infiltration.

4.3.4 Ultrasonic Infiltration of Aluminum in to Carbon Fiber

Ultrasonic infiltration was tested with coated and uncoated Toho G30 fibers and Hexcel IM7 fibers using a pure aluminum melt with a small magnesium addition. The infiltration was achieved using an ultrasonic source operating at 1500 W and a nominal

frequency of 20 kHz. The system consisted of a control box connected to a converter/probe couple that was used to convert electrical signals to vibration. The converter consisted of an air-cooled titanium shell enclosing a piezoelectric transducer. The probe, bolted to the converter shell and driven by the transducer, was a tapered piece of titanium approximately 12 inches in length, used for immersion in the aluminum melt.

The probe was inserted approximately 2 to 3 inches below the surface of the aluminum melt. This level of immersion is not necessary for infiltration - other research involving ultrasonic infiltration has used immersion levels of under 1" [20]. However, it was necessary to heat to probe to 750°C in order for it to oscillate at the appropriate frequency and this was only obtained through immersing the probe several inches in to the melt. The unfortunate drawback of having to heat the probe is that the converter, being directly attached to the probe and so close to the metal melt, was subjected to significant radiative and conductive heating. This would cause overheating and failure of the converter.

Another unfortunate consequence of having the probe extend so far in to the aluminum is that the metal rapidly corroded the probe. The probe would be noticeably smaller in size after only 30 minutes of use. Oxidizing the probe in air at 1000°C and coating its surface with boron nitride helped to alleviate this problem.

Prior to reaching the melt, fibers for ultrasonic infiltration were preheated to approximately 450°C in a tube furnace. This measure was to burn off the fiber sizing and reduce the amount of aluminum frozen to the fiber surface. After preheating, fibers were drawn through the melt and under the ultrasonic probe at a rate of 0.2 – 0.5 feet/sec for 3K size fiber yarns, and slower for the 12 and 24K yarns. Faster speeds are preferable to

reduce fiber oxidation and carbide formation, but larger yarns are cheaper and less labor-intensive for large-scale production. Drawing at too fast of a speed results in incomplete infiltration. Toho G30 fibers (3K and 24K) and Hexcel IM7 fibers (12K), both PAN-derived, were successfully infiltrated with aluminum using this method, producing several meters of precursor filament approximately 1mm in diameter. Ultrasonic infiltration was also carried out on fibers coated with aluminum oxide and zirconium oxide, but only those coated with aluminum oxide produced usable samples. G30 fibers that were pre-coated with nickel could not be infiltrated – they would burn just prior to contact with the matrix.

After infiltration, the infiltrated fibers were wound about a spool of approximately 2 feet in diameter. They possessed a non-uniform cross-section, as there was no convenient way to heat a die through which to draw the composite after infiltration. Attempts at using an unheated die caused metal and slag to solidify about the die opening, which would then block the opening and break the composite.

4.4 Tensile Testing Results and Discussion

Tensile testing of the composite samples was conducted at Georgia Tech's Mechanical Properties Research Laboratory. In order to provide a ductile surface for gripping the sample, copper tubing was glued over the ends of each sample (Figure 23) using a 2-part epoxy and allowed to cure for at least 24 hours. Care was taken to ensure that the sample was mounted true in the tubing and that the epoxy formed a smooth transition between the end of the copper tubing and the beginning of the sample, so as to

minimize any stress concentration. Two beads of silicone caulk were placed on each sample to provide a non-slip surface for the knife-edges of an MTS ½" extensometer. All samples were tested in an MTI Phoenix 1000 lb. load frame at 0.1 inches/min. Samples were initially attached the the test frame using pressurized-air grips to minimize the chances of breaking the sample during mounting. However, these did not provide enough grip force, even, when the sample was sandwiched between two sheets of silicon carbide sandpaper. Mechanical grips were used for the majority of the tests, even though several samples broke during mounting. Samples broken in tension were mounted in an aluminum tube and held in place with a setscrew. This allowed for viewing of the fracture face using a Leica inverted microscope. Fracture face area was calculated using the ImagePro software. In certain cases where the fracture face contained too much topography to allow focusing of both the fibers and the fracture face, area and fiber volume fraction were obtained from a polished cross-section of the sample (Figure 22). It can be seen from this figure that many of the pores between fibers are on the order of 1-2 μm in length, far smaller than the 14 μm used in the example in Section 2.1.1. The IM7 samples had a consistent volume fraction of around 30%, while the G30 samples had volume fractions between 39-50%.

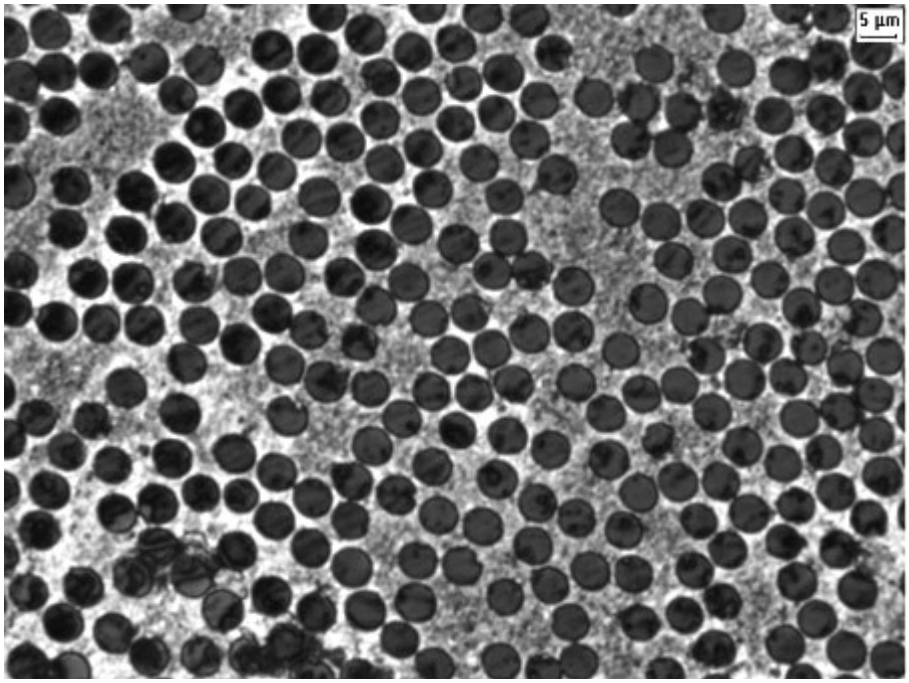

Figure 22: Polished cross-section of composite with aluminum oxide-coated fibers

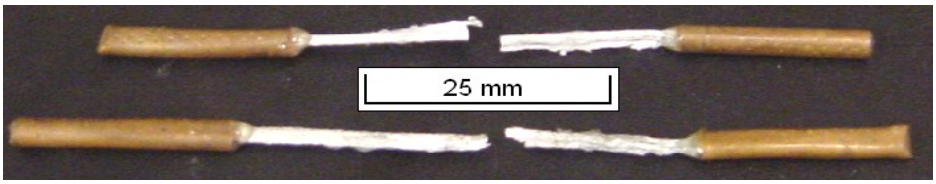

Figure 23: Broken composite samples mounted in copper tubing

4.4.1 Strength data

Below in Table 1 are the average tensile strength data, and their calculated rule of mixtures values. The data are averaged over at least five tensile tests per sample type. The ultimate strength and strain of the composites are poor, but this is very likely the

result of poor processing conditions rather than any fundamental incompatibility between constituents.

Table 1: Average mechanical properties of several composite specimens

Type	Modulus (GPa)	% ROM	Strength (MPa)	% ROM	Strain	Volume Fraction
IM7+aluminum oxide	72.4	57%	572	35%	0.40%	28.10%
IM7	94.9	73%	606	36%	0.90%	29.40%
G30	28	21%	255	15%	0.80%	40.50%

Because the infiltration process was manually controlled, there were myriad factors that were not optimal. One of the more important factors is that, as mentioned previously, the composite samples were immediately wound about a spool following emergence from the aluminum melt. This means that they solidified in a curved shape rather than a straight one, and that tensile testing imparted significant bending forces on the sample that would cause it to fail prematurely. Also, because the composites were not drawn through any sort of die prior to spooling, these samples possessed many surface defects and irregularities in cross-section that could act as stress concentrators. Die drawing would potentially have increased the mechanical properties of the composites by eliminating spread in the fiber tow as it was fed in to the metal bath. This spread contributes to gas entrapment, causes excess metal pickup and creates non-uniform exposure to ultrasound intensity.

It is also possible that the fiber coating was not uniform about the fiber. Defects in the coating could lead to stress concentrations or the formation of carbide. This could explain the much lower fracture strain of composites with coated fibers.

4.4.2 SEM analysis

To obtain a better understanding of the causes of poor mechanical properties in the composite samples, their fracture faces were examined with a LEO 1530 SEM. Typical fracture faces are visible in Figure 24 through Figure 26. The fracture faces look good. The matrix has pulled away from the fiber as expected, and the fibers do not appear to have undergone any degradation. Regardless of type of fiber or coating presence, the composites are all very well infiltrated and have a strong fiber/matrix interface: there is almost no fiber pullout, and where pullout has occurred it is of low magnitude. As mentioned earlier, a strong interface is not necessarily desirable; interface strength is not a metric for interface quality. With the range of coefficients of thermal expansion present in carbon fiber-reinforced aluminum, composites may suffer from too strong of an interface and be exceedingly brittle. This seems quite likely, given the extremely low failure strain.

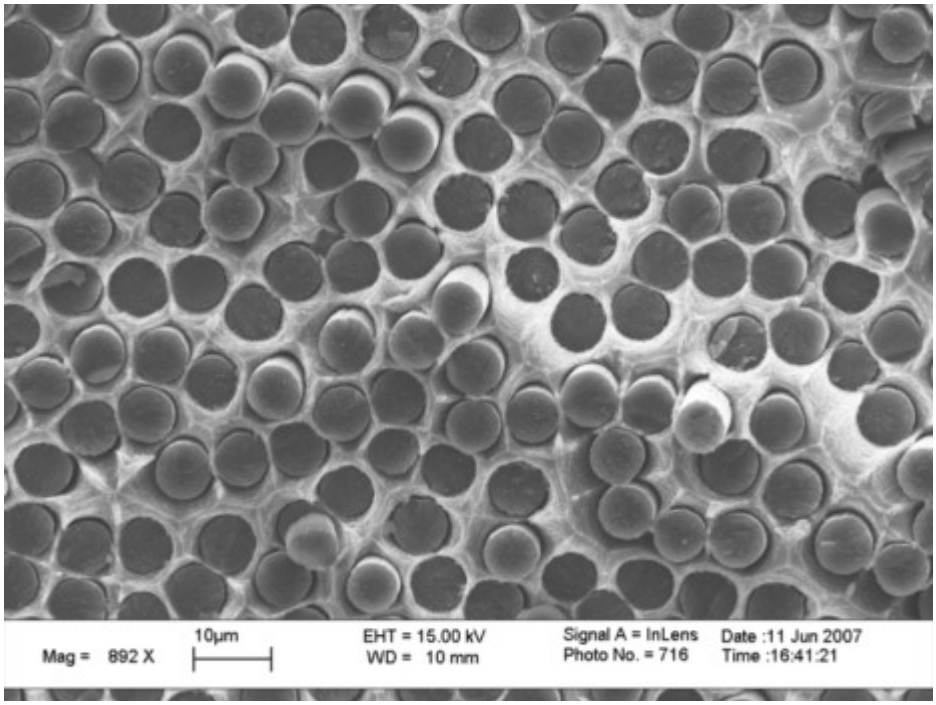

Figure 24: Fracture face of G30/Al composite sample broken in bending.

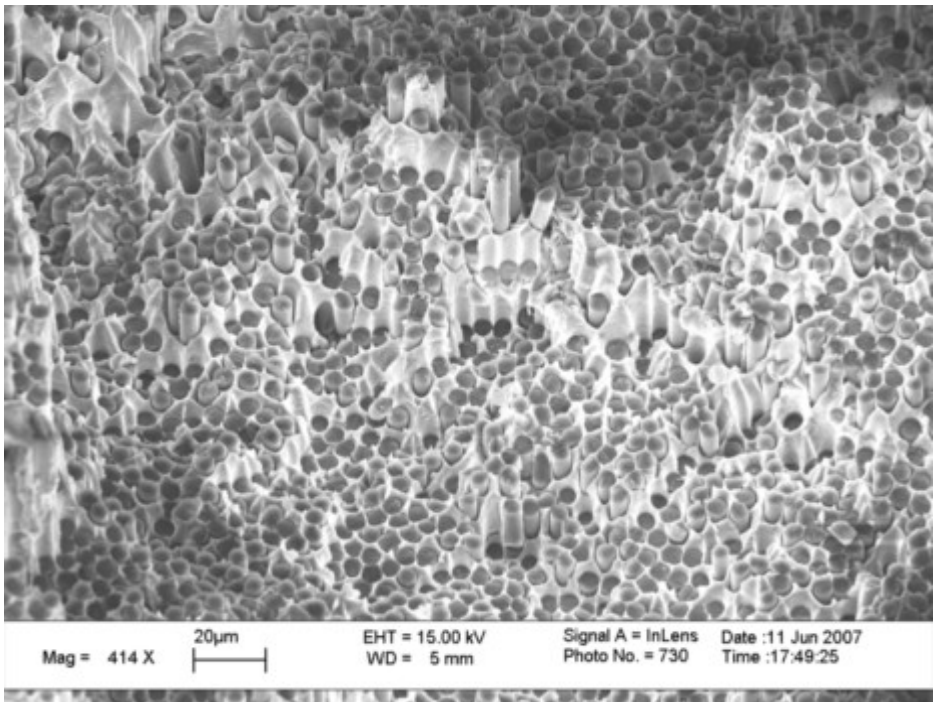

Figure 25: Fracture face of composite sample at 30° angle. Fibers are IM7 with aluminum oxide coating

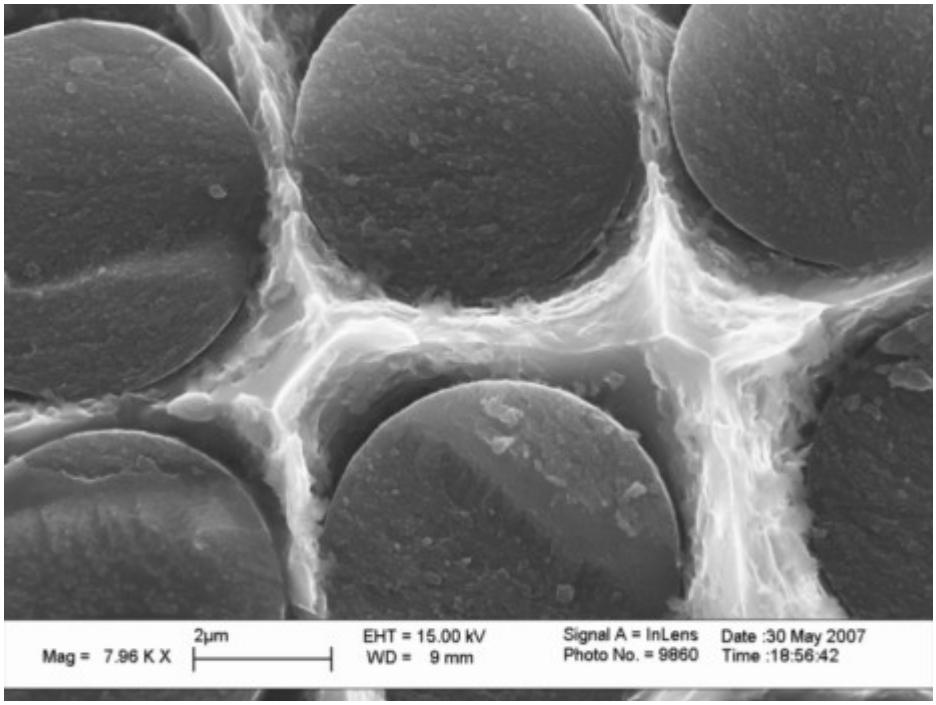

Figure 26: Well-infiltrated fibers in Al-IM7 composite sample. Sample was broken in tension.

Perhaps the most interesting features of the composites are the defects within them. As stated previously, voids are one of the significant issues to be dealt with in ultrasonic infiltration, and these composites are no exception. Each possesses a sizable void fraction, visible in Figure 27 and Figure 28. These regions seem to be scale with fiber tow size, as an infiltrated tow of G30 fibers in 24k yarn shows a drastic increase in void volume (Figure 29).

Voids are thought to contribute to the poor mechanical properties of the composites, as the matrix in this region is clearly unyielded, and is not contiguous. Noncontiguous matrix prevents fiber/matrix load transfer, and reduces the amount of area available for load bearing. Voids can also act as points of origin for cracks [20]. Perhaps some of the most compelling evidence for void degradation of mechanical properties is

the fact that the voids are easily imaged. This means that they are not only present in sufficient quantity throughout the sample, but also that the composites are breaking along planes occupied by voids.

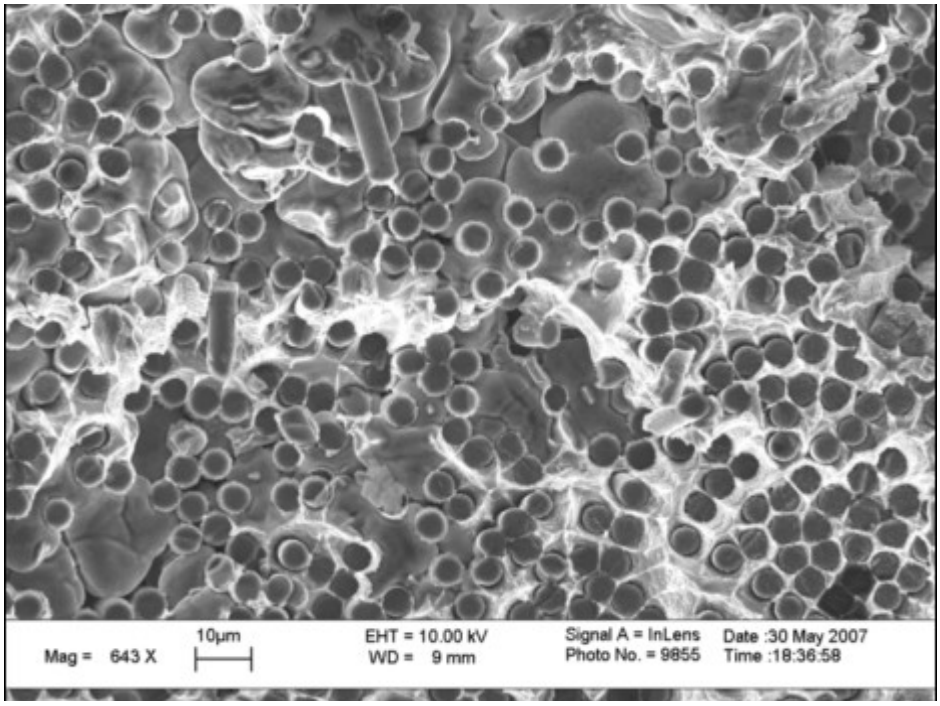

Figure 27: Void region in coated fiber composite. Region occupies approximately the left two-thirds of the image, and displays a structure similar to that in Figure 6.

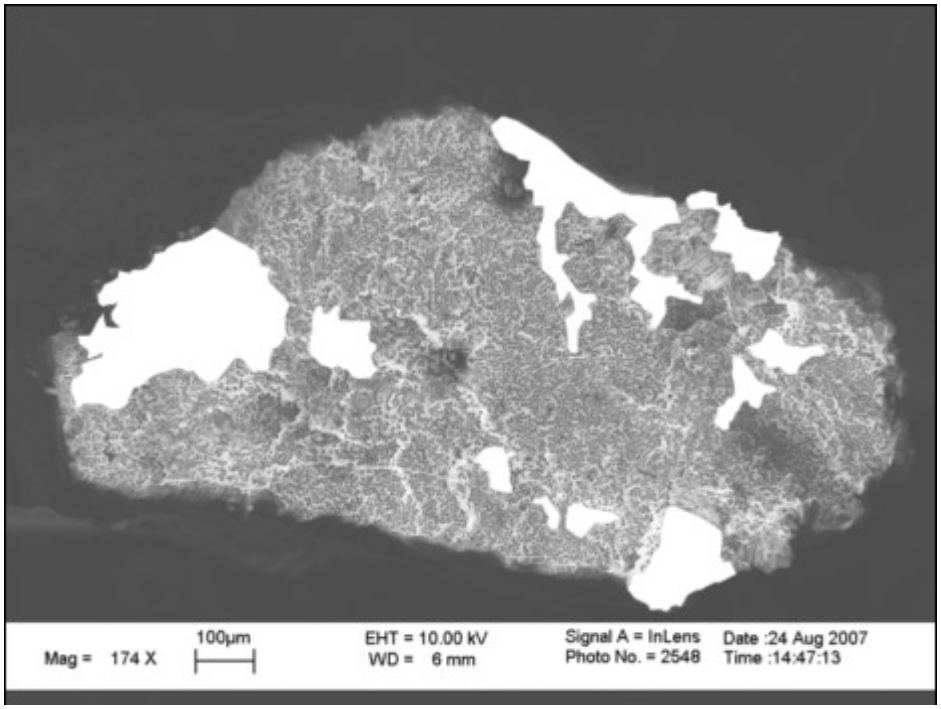

Figure 28: Al-IM7 composite cross-section. White regions represent void areas.

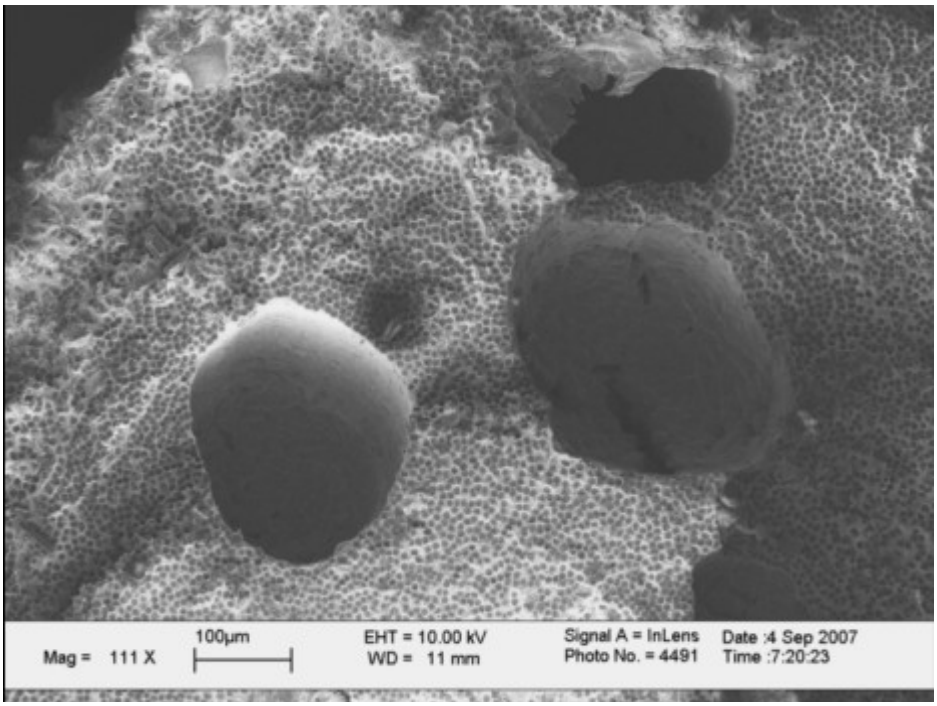

Figure 29: 24k tow of G30 fibers infiltrated with aluminum, with significant void fraction.

Closer examination of the voids reveals that they are the only region where the fiber coating is present. In a typical fracture face, such as in Figure 30, there is no discernible difference between coated and uncoated fibers. It is only in void regions, such as in Figure 31, that one can clearly identify a fiber coating. This coating is composed of aluminum oxide, as it should be, and this result is confirmed by elevated Al and O peaks in EDXS spectrum of the coating region (Figure 32 and Figure 33), as compared to drastically lower Al and O peaks in spectra of the bulk matrix and even the matrix that has pulled away from the fiber surface.

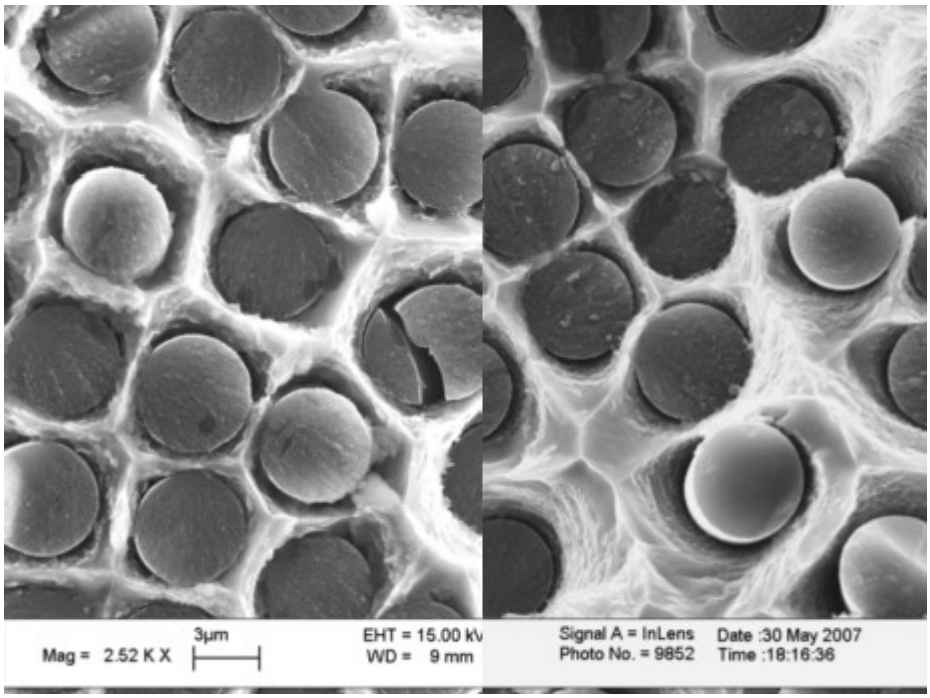

Figure 30: Identical fibers: Al_2O_3-coated on the left, plain IM7 on the right

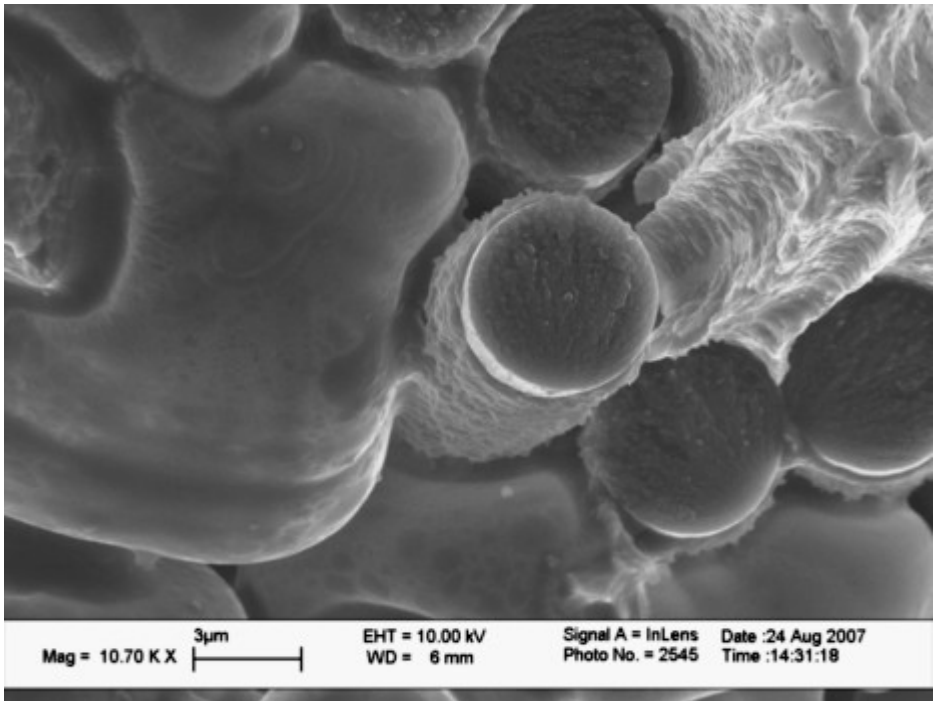

Figure 31: Coated fiber in void region

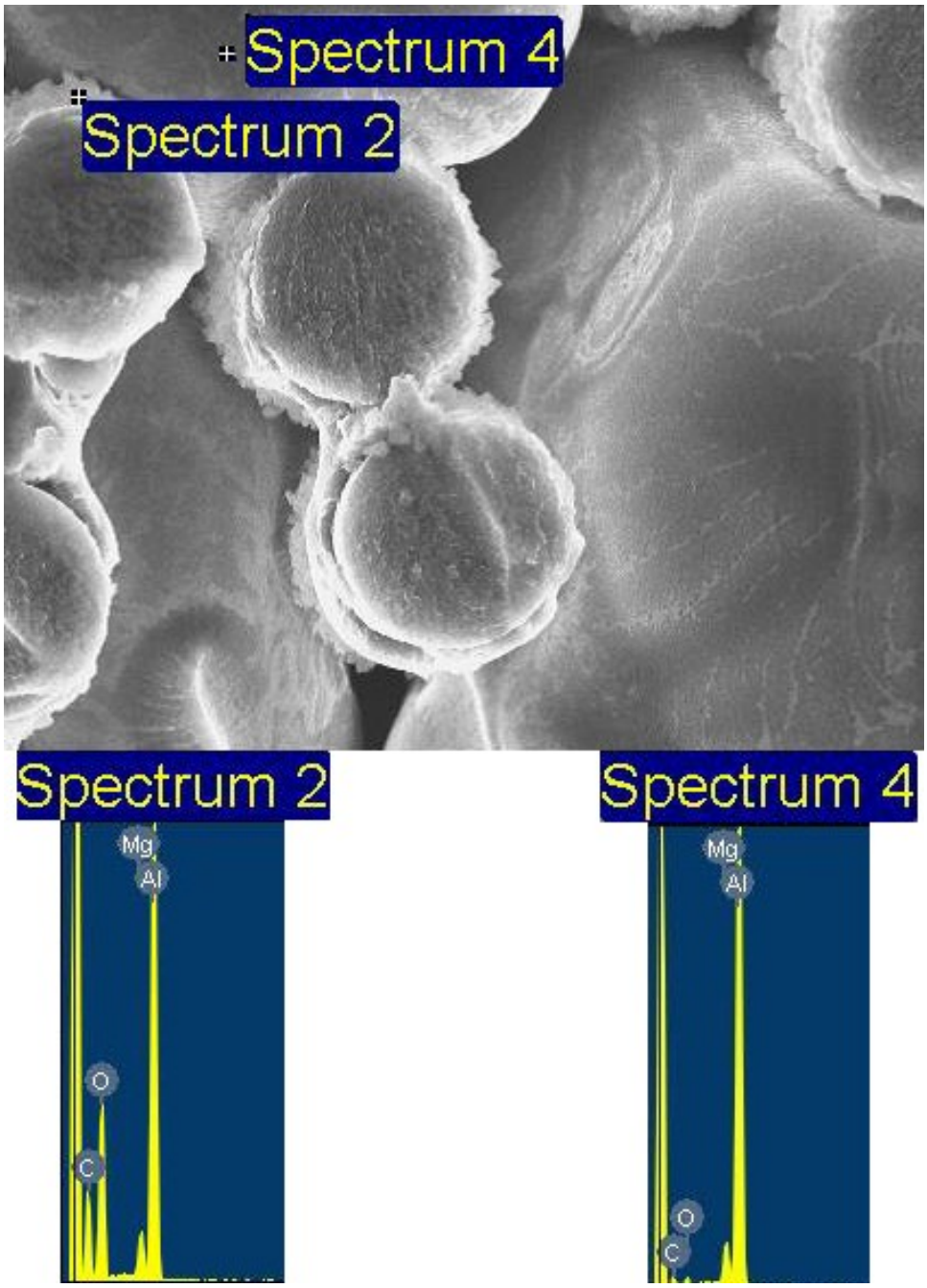

Figure 32: EDXS spectra of: 2) fiber coating 4) bulk matrix

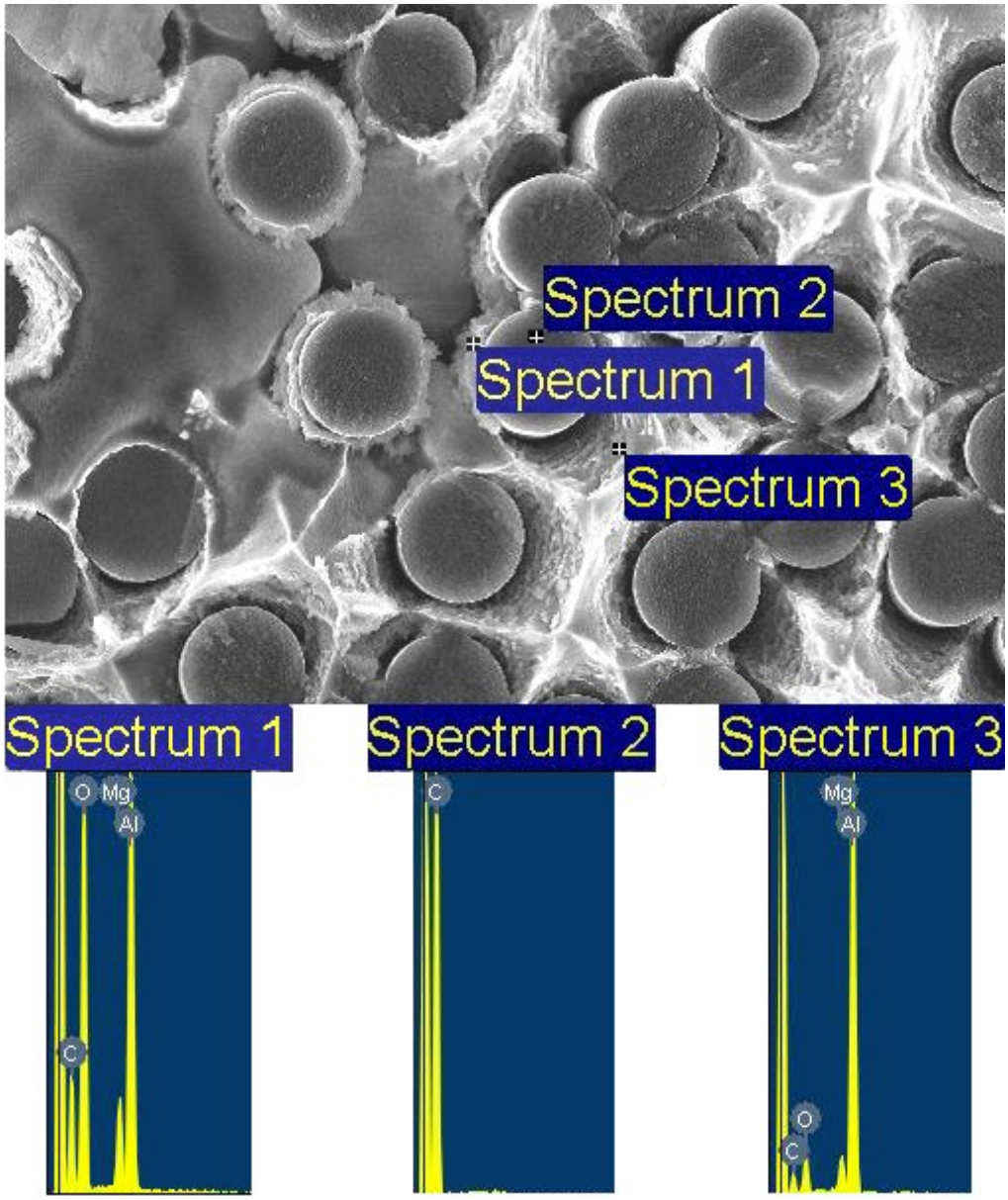

Figure 33: EDXS spectra of: 1) fiber coating 2) fiber along its axis 3) matrix pulled away from fiber. Each fiber diameter is 5.2µm.

Somehow the coating was not being fully included in the final composite. There are several possibilities regarding the cause of this, and its true origin has not yet been determined. What is known is that the void regions contain entrapped gases that can cushion against temperature and stress. Gases are better thermal insulators as compared to solids or liquids, and because they can undergo volume changes, they can compress or

expand in response to a stress and shield any components contained within the void. This could imply several possibilities about fabrication conditions elsewhere in the composite. It is possible that the thermal stress of the cooler fibers being immersed in the aluminum was enough to crack the coating and cause it to be washed away on metal contact. This is indeed a risk with any ceramic coating, but even more so with an inert oxide coating. Perhaps the coating is so weakly present about the fiber that even if it survived the thermal stress, the fluid flow of the metal was enough to displace it. It is also possible that the cavitation induced by the ultrasound was enough to shed the fiber coating.

4.5 Carbon coating

The removal of the aluminum oxide coating prompted a reevaluation of what constituted a good fiber coating, as the interface between the fiber and coating was, until this point, far less important than the interface between fiber and matrix or between coating and matrix. The oxides were chosen as coating materials not only of their ease of manufacture, but also because of their insulating and possible wetting properties. Use of a different type of coating would require a completely different processing step, and would not give the same potential corrosion benefits of an insulating coating, as both the carbides and metallic coatings are electrically conductive.

Katzman [50] encountered a similar problem in trying to develop magnesium matrix composites reinforced with graphite fibers that had been coated with silica, a rather analogous situation to our attempt at oxide coated fibers in a reactive light metal matrix. Katzman's attempts at dip-coating silica-coated fibers into a magnesium matrix

would work for many fiber types except those of higher modulus – those fibers would retain very little magnesium. He found that the coating was being removed upon contact with the magnesium matrix, and attributed this to differences in surface morphology of the higher modulus fibers.

On a microscopic level, carbon fibers consist of several graphite planes of varying orientation. As graphite planes become more well-oriented along the length of the fiber, fiber modulus increases [59]. Plane orientation also determines the reactivity of the fiber, because a graphite plane is chemically active only on the plane edge, where dangling bonds are present [60]. Several studies [60][61][11] correlate these reactive sites with carbide formation, and plane edge exposure and geometry depends on the specific fiber. Several common fiber orientations are visible in Figure 34.

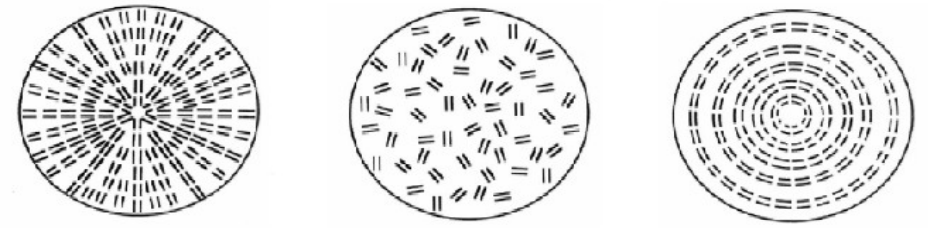

Figure 34: Common graphite plane orientation in fibers: radial, random, onion skin

Since it is possible that the fiber surface contains very few exposed plane edges, Katzman's solution to this problem was to develop a reactive amorphous carbon coating for these low-reactivity fibers. The coating is applied by a solution of 10-40 g/L of petroleum pitch dissolved in toluene. Fibers are coated with the solution, and then pyrolyzed at temperatures up to 550°C in an inert environment. The resultant coating is

approximately 20 nm thick (Figure 35), and is reactive enough to maintain adhesion between the fiber and its oxide coating.

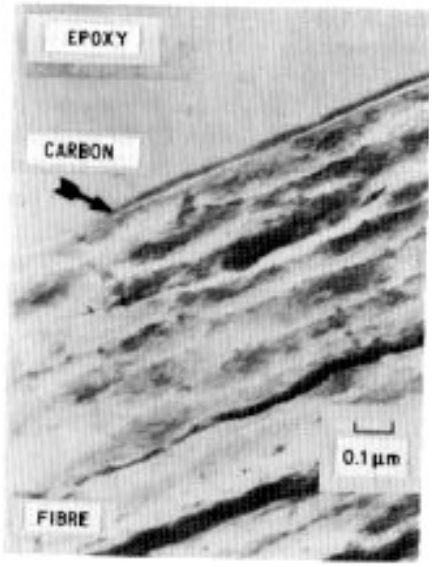

Figure 35: Amorphous carbon coating deposited by asphalt-toluene solution. From [50].

Lacking any data concerning the layout of the graphite planes within the IM7 fibers and G30 fibers used in infiltration, the fracture face is the only resource available to determine graphite plane orientation. Most of the IM7 fibers seem to display planes that originate at a single point on the fiber, shown in Figure 36. A schematic of the graphite plane orientation, and their convergence to this point is illustrated in Figure 37. If one extrapolates that trend to the planes at the fiber surface, very few plane edges will be exposed and the fiber will be nonreactive. Some of the G30 fiber display a similar pattern to the IM7 fibers, but they are not nearly as consistent.

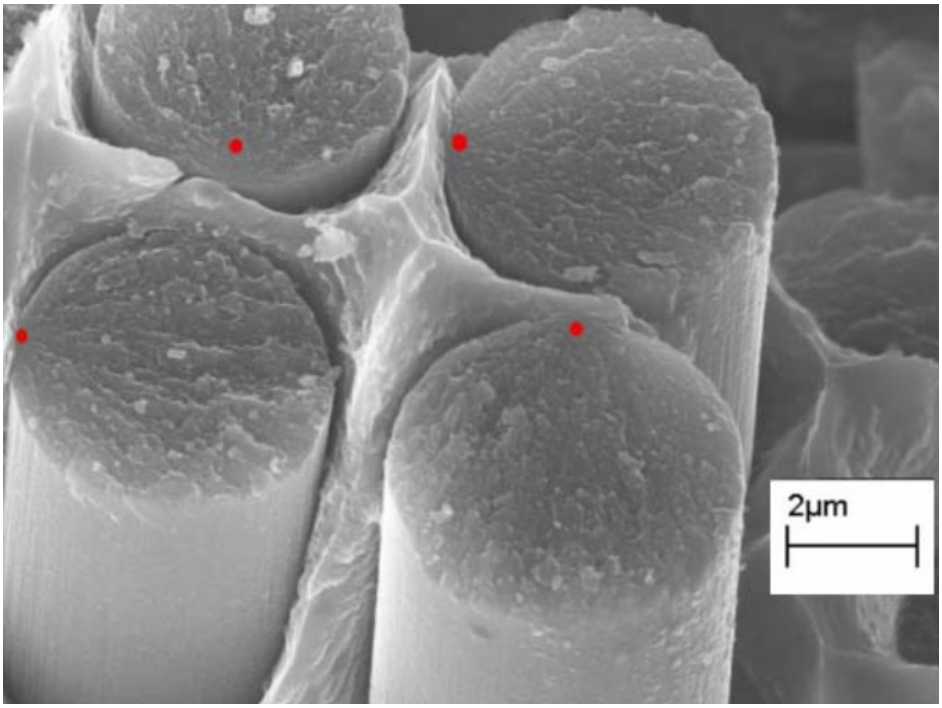

Figure 36: Fractured IM7 fibers and their points of convergene for graphite planes

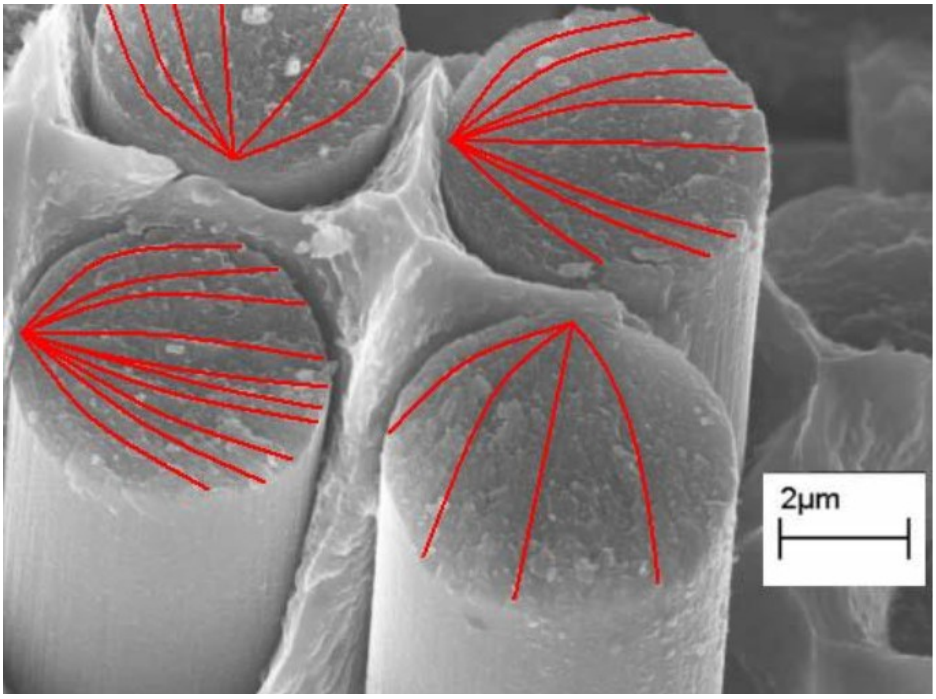

Figure 37: Schematic illustrating possible arrangement of graphite planes.

4.5.1 Coating and testing procedure

IM7 fibers were coated using a solution of approximately 37 g/L asphalt (Dykes Paving, Norcross, GA) dissolved in toluene. Each fiber tow was dipped in to the solution for 30 seconds, and slowly removed. Several small fiber samples of approximately 1.5 cm in length were dipped in this solution and pyrolyzed at different heating schedules to observe the evolution of the coating process under SEM. The fiber samples were explicitly cut to length after their dipping so as to expose any coating interface. Fibers were pyrolyzed at 300°C, 550°C and 800°C. A single fiber sample was coated and pyrolyzed twice at 550°C. Each sample was pyrolyzed in a TA Instruments Q50 TGA. Pyrolysis was conducted under nitrogen flow of 35 mL/min, at a heating rate of 10°C/min. Each sample was equilibrated at its set-point temperature for 10 minutes.

Three fibers tows of approximately 2 m in length were coated for infiltration studies. Because infiltration was conducted at another facility, these fibers had to be sent through the mail. In order to minimize damage to the fibers from handling, each tow was wound about a glass pipette and then dipped in the asphalt solution. They were pyrolyzed in a mullite tube furnace at a temperature of at least 400°C. The exact temperature is unknown, as the samples produced significant amounts of smoke at temperatures near 425°C, and they were moved to a cooler zone of the furnace tube to prevent further smoke release. The precision of heat treatment temperature does not seem particularly important, given that asphalts and pitch products vary in composition depending on feedstock [62]. Furthermore, Katzman's patent [63] describes the pyrolysis as being

conducted at any temperature from 350°C to 450°C, and his paper [50] even makes allowances for up to 550°C.

Two of those fibers tows were then dip-coated with the aluminum nitrate and urea solution used for producing aluminum oxide coatings. Because of the fragility of that coating, these fibers were heat treated to produce the oxide coating only after they had been received at the infiltration site. Each tow was then infiltrated according to the procedure described in Section 4.3.4. Infiltration was more difficult with these fibers, but it produced two samples of approximately 80 mm in length. Each was much less uniform (Figure 38) than even previously produced samples, as the winding of the tows on the pipette caused them to flatten and spread. Only one of these samples was successfully broken in tension, per procedure described in Section 4.4.

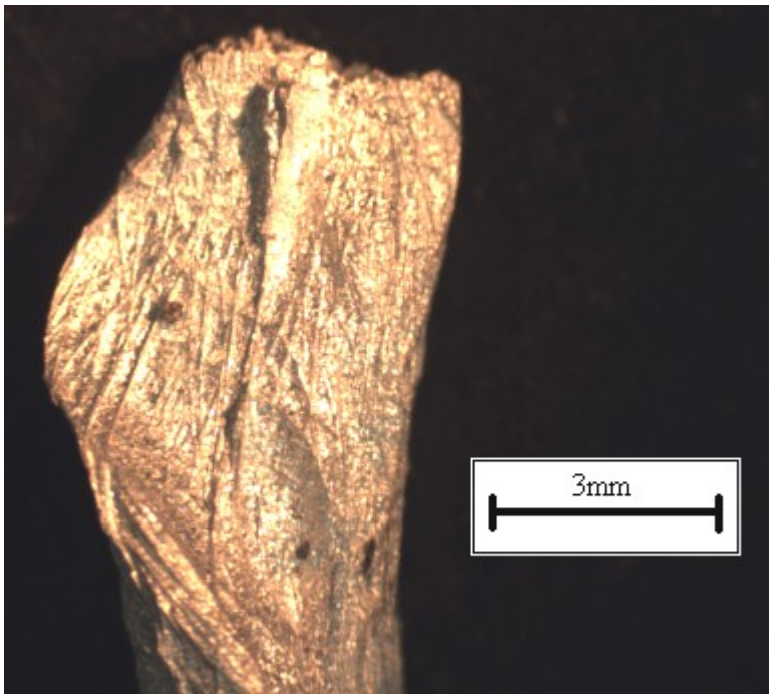

Figure 38: End of composite sample with asphalt-coated fibers. Spread in the fiber tow has been maintained in the final shape.

4.5.2 Coating results

Figure 39 displays the asphalt solution as deposited on the fiber surface, with no pyrolysis. Fibers are clearly stuck to one another, as would be expected from the evaporation of the toluene solvent and remaining asphalt residue. They began to separate from one another for coating temperatures of 300°C and 500°C, visible in Figure 40 and Figure 41 respectively, but still remained noticeably adhered. At 800°C, the fibers showed significant deterioration, despite the fact that they were in a nitrogen atmosphere. It is possible that they were not given sufficient time to cool in this atmosphere, but it is not of great concern, as this temperature is neither practical nor likely encountered.

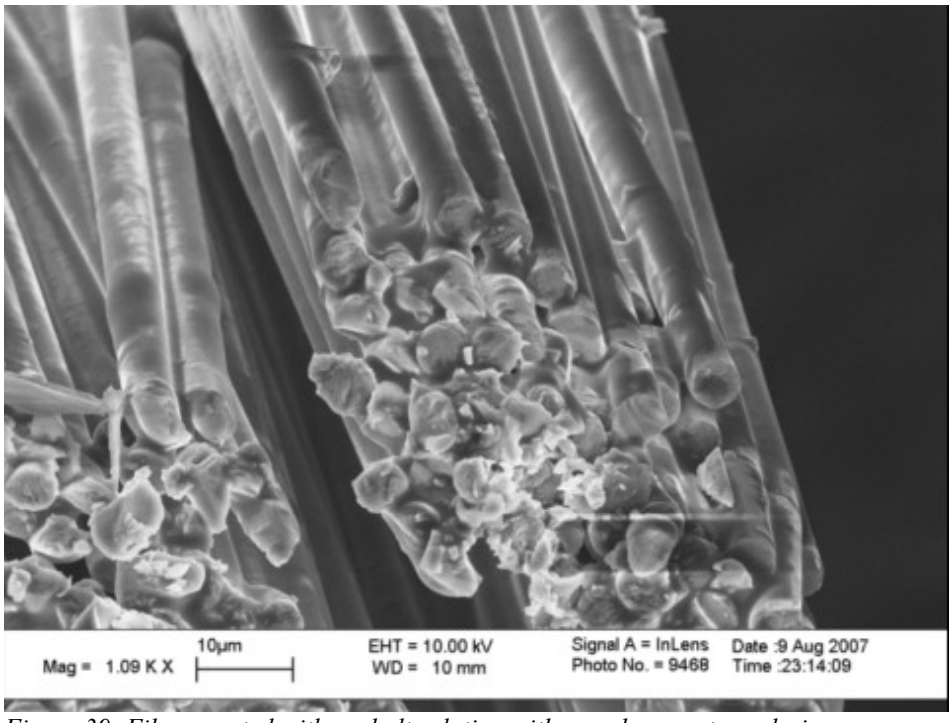

Figure 39: Fibers coated with asphalt solution with no subsequent pyrolysis.

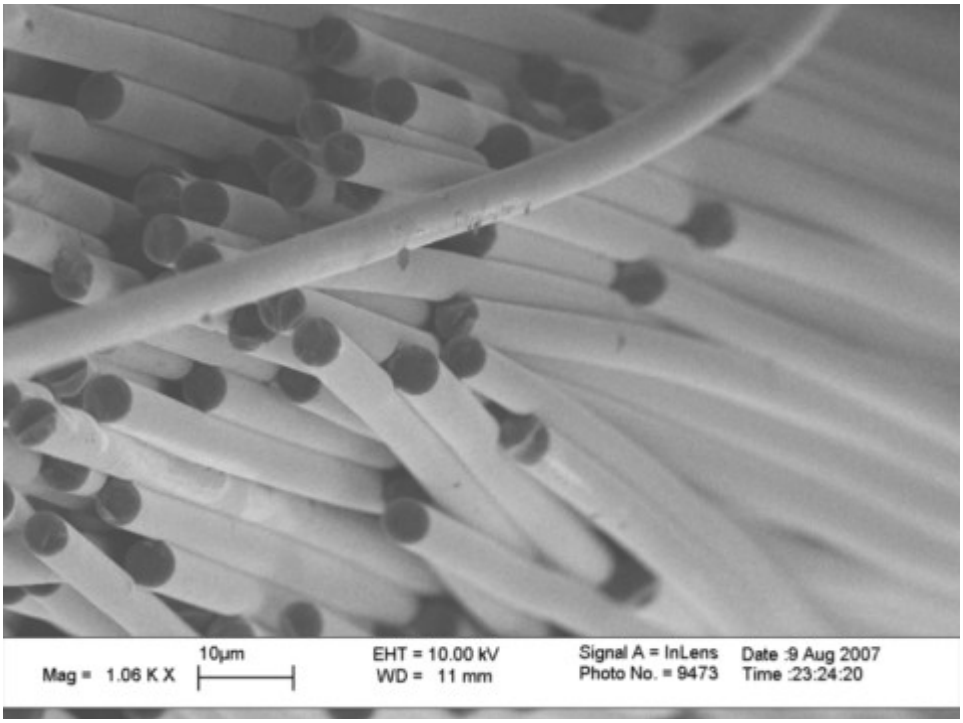

Figure 40: Asphalt-coated fibers pyrolyzed at 300°C.

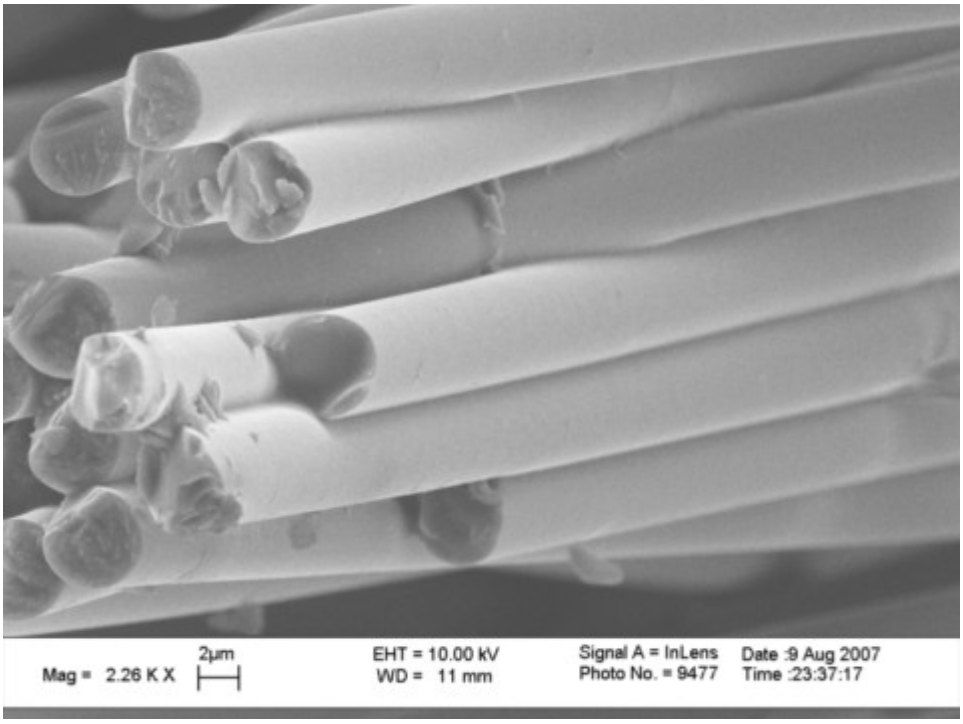

Figure 41: Asphalt-coated fibers pyrolyzed at 550°C.

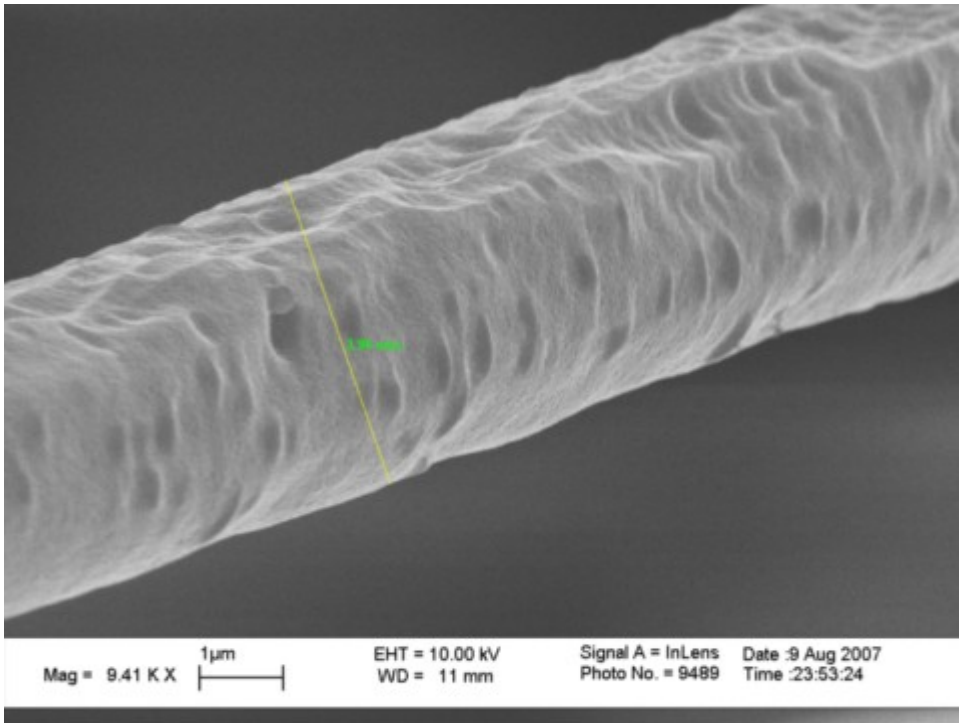

Figure 42: Asphalt-coated fibers pyrolyzed at 800°C. Fiber diameter has shrunk from 5.2 µm to 3.96 µm.

It was hoped that some coating interface could be viewed without having to examine the sample under TEM. There is obviously something on the fiber surface, but the interface allows for a distinction of what is the fiber and what is the coating. Although the fiber coating produced by Katzman was only 20 nm thick, he did not specify the concentration of asphalt used in achieving 20 nm thick coatings. It is possible that 20 nm is a lower end of coating thickness, and a coating of thickness 80-100 nm would be easily imaged. However, no interface was readily apparent in the SEM analysis. It is clear that both coatings produced at 300°C and 550°C are lighter in color along their length as compared to the fiber end. Brightness is usually correlated with low electrical conductivity, as those regions are unable to disperse incident electrons. This is probably not sufficient evidence, as the conductivity of amorphous carbon depends very much on

its structure and doping, both of which are unknown. Perhaps the best evidence of the coating presence lies, much like with the zirconia coating, in its defects. Fibers are clearly still attached to one another in coatings pyrolyzed at 550°C (Figure 41), and that may be the best indication of a coating achievable with the SEM. Not even the sample coated twice (Figure 43) provided a coating thick enough for interface analysis, and the spread in fiber diameter was too great (Figure 44) to attribute any fiber thickness change to coating presence.

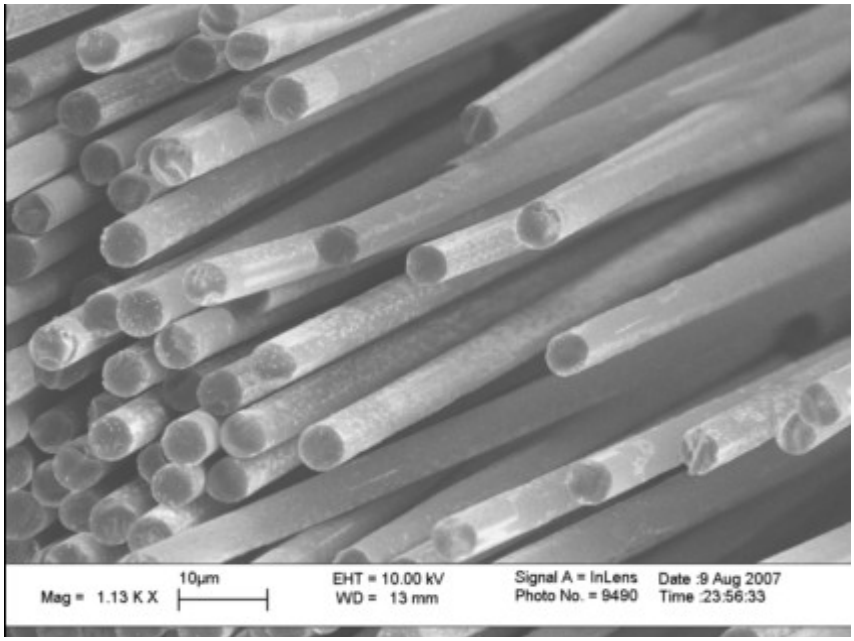

Figure 43: Fibers that have undergone the coating/pyrolysis process twice, to produce a thicker asphalt coating.

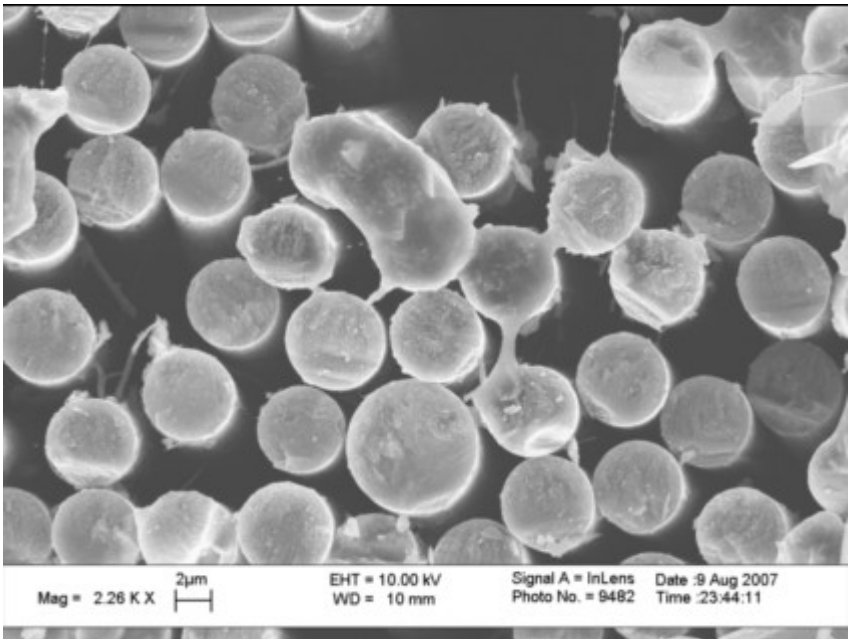

Figure 44: Variance in fiber diameter.

The only infiltrated sample successfully tested in tension broke at a load of 422 N (95 lbs). This is close to the highest load experienced by any of the other samples, but the area of the asphalt-coated fiber composite sample was 1.82 mm^2, a value nearly double that of the other samples. Such a large area means that the actual stress borne by the sample was only 231 MPa (33.5 ksi). Because the same amount of fibers were present in the sample, a larger area means a smaller fiber volume fraction. 231 MPa equates to a rule of mixtures strength of 27%. Analysis of the sample fracture face revealed that the composite possessed a significant amount of large air bubbles, in addition to the uninfiltrated regions present in many of the other samples. These bubbles are visible in the fracture face in Figure 45 and are highlighted in Figure 46. They occupy 23.8% of the area of the fracture face.

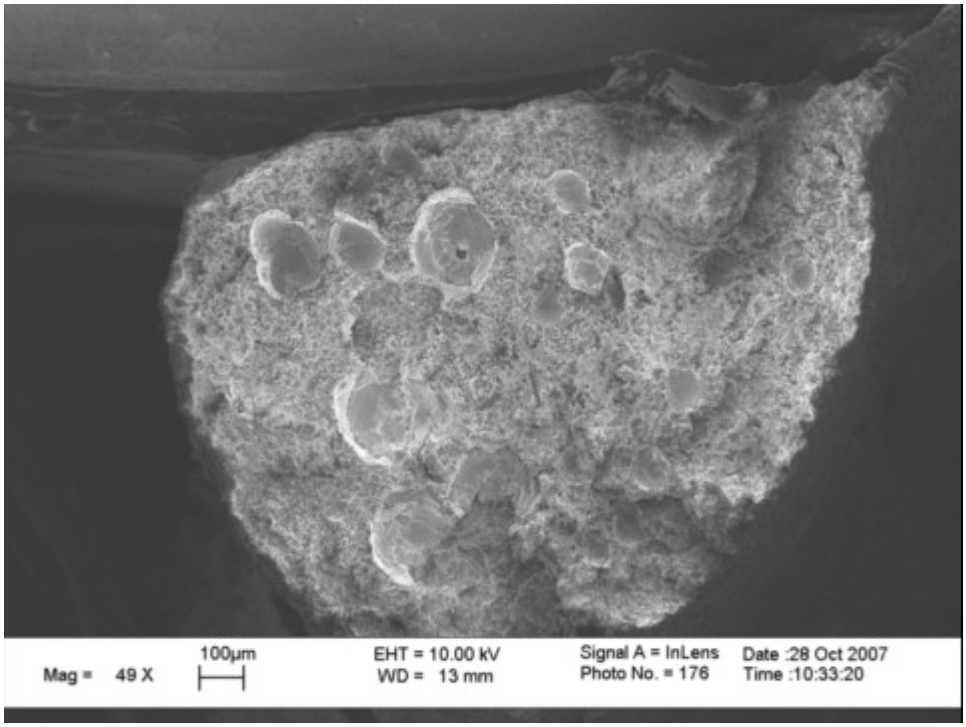

Figure 45: Fracture face of broken composite sample with asphalt-coated fibers. Area is 1.82 mm^2

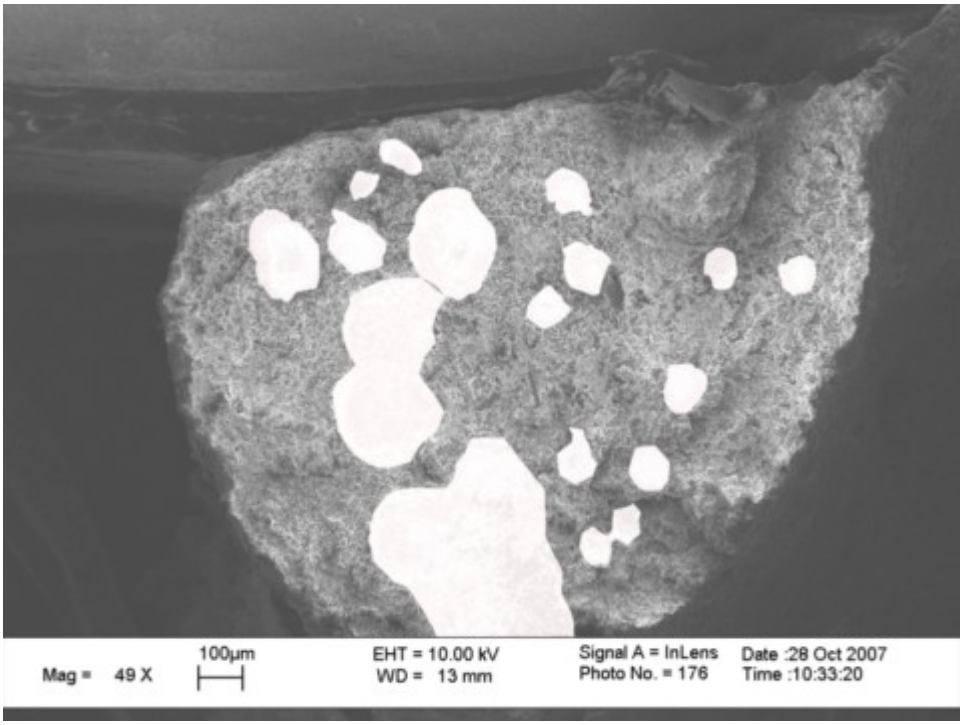

Figure 46: Fracture face with bubble area removed. Bubble area occupies 23.8% of the total area.

In highlighting bubbles, only those regions displaying specific bubble "morphology" - areas with a characteristic "crater," or spherical cut-out – have been highlighted. The composite also features many uninfiltrated regions similar to those present in other samples. These regions are characterized by a large area of globular, unyielded matrix with almost no fibers present. If all void areas, being bubbles and general uninfiltrated regions, are included, the remaining area of "good" composite is significantly smaller (Figure 47). Such regions occupy a total of 57% of the composite cross-sectional area. If these areas are not considered to bear any load (ultimate strength of aluminum is 1.6% the ultimate strength of the fibers), nor assist in load transfer between fibers (no fibers present in void regions) then the stress borne by the remaining area of the composite would amount to 541 MPa (78.4 ksi), for a rule of mixtures strength of 29%. Such a number is more in line with tensile data from other samples, but it should be noted that it is probably low, as the bubbles will act as stress concentrations, significantly reducing the tensile strength from that of a void-free composite.

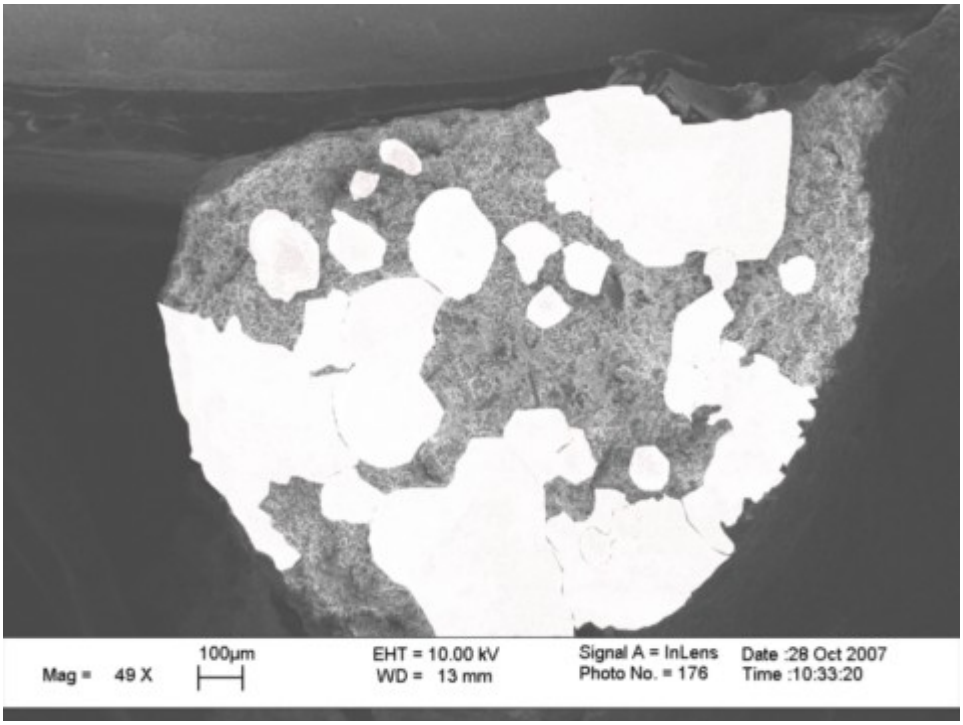

Figure 47: Composite fracture face with all bubbles and general void regions removed. These regions occupy 57% of the total area.

The interfaces of the asphalt-coated fiber composites are their most interesting feature. A micrograph of the composite fracture face is visible in Figure 48. It looks rather plain, except when compared to the standard composite interface, such as in Figure 26 or Figure 30. The fiber/matrix interface is markedly stronger with asphalt-coated fibers as compared to other samples. This can be evaluated by the reduction of matrix separation from the fiber at the fracture face. Matrix separation from the fiber is still visibly occurring, but to a lesser extent. This could be the result of a discontinuous asphalt coating.

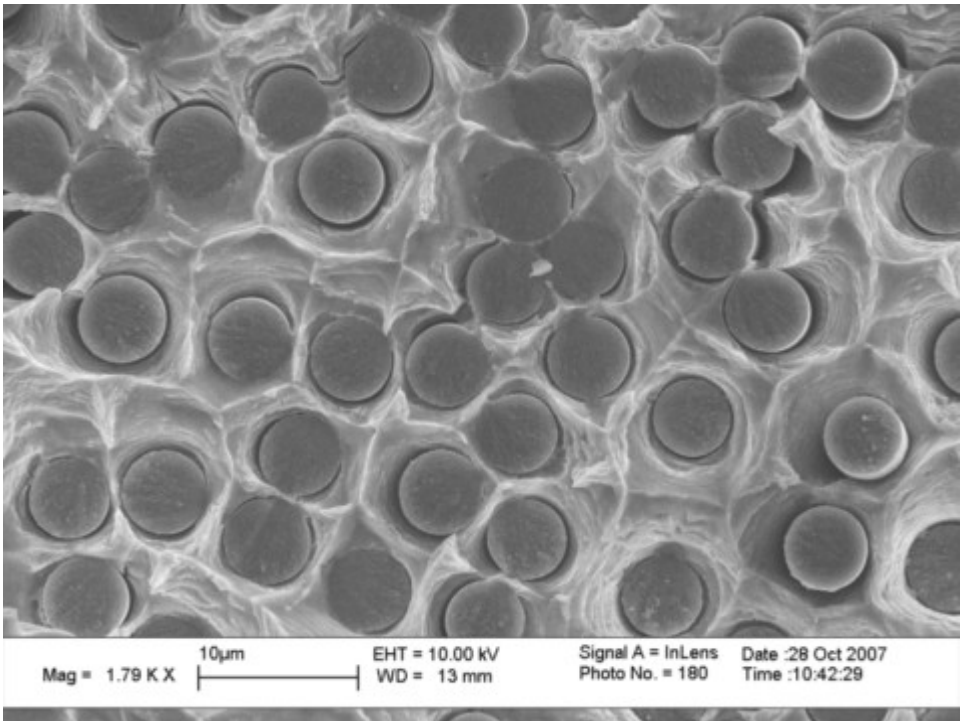

Figure 48: Fracture face detail, showing stronger fiber/matrix interface.

Also present in these composite samples is a characteristic not seen in any of the other samples: many transverse cracks that propagate through both the matrix and the fiber (Figure 49 and Figure 50). Previous samples broken in tension have never displayed fiber cracking, let alone cracking of any sort normal to the direction of applied stress. Such cracking indicates that, the fiber/matrix interface is stronger than the transverse strength of the fiber, or else the matrix would have separated from the fiber and yielded.

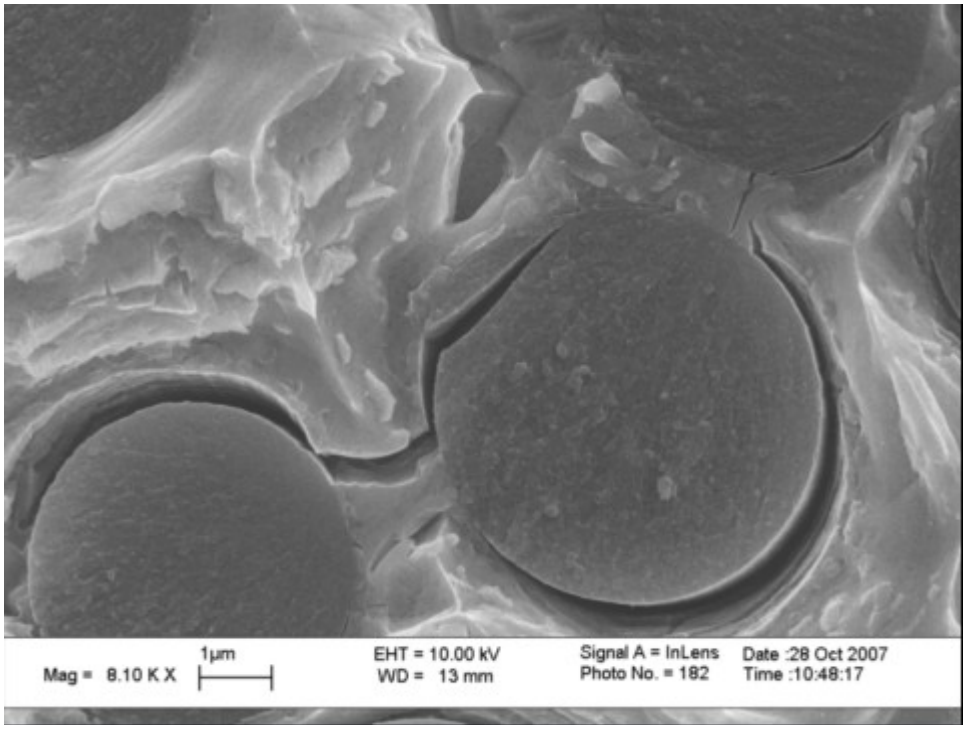

Figure 49: Transverse cracking in asphalt-coated fiber composite

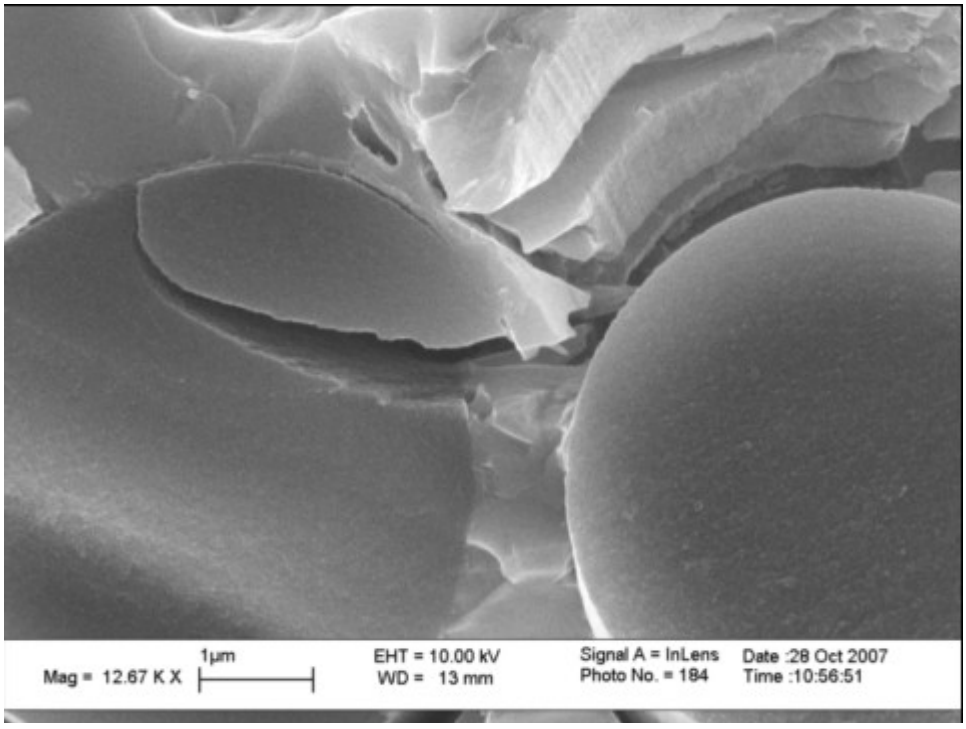

Figure 50: Detail of transverse cracking in asphalt-coated fiber composite.

However, once again the bulk of these fibers do not display any of the aluminum oxide coating that was deposited on them. Only in the void regions is any evidence of the coating visible, indicating that the asphalt has not promoted oxide adhesion to the extent necessary. Below in Figure 51 are fibers that are at the edge of one of the bubbles in the fracture face of the composite sample. They can be seen to have a rough layer about their surface. This layer is examined in closer detail in Figure 52. The coating on the center fiber can be seen to be cracked, and partially removed, and aluminum metal can be seen to the left of the fiber, mixed with the oxide coating. This effect is visible in higher detail in Figure 53. Additionally, the coating appears to be washing off of the leftmost fiber of Figure 52. This fiber has no fibers to its left, so the particulate coating on the surface of the aluminum can only originate from the leftmost fiber in the micrograph. These micrographs seem to indicate that it is the fluid turbulence that is responsible for the coating removal, rather than the cavitation.

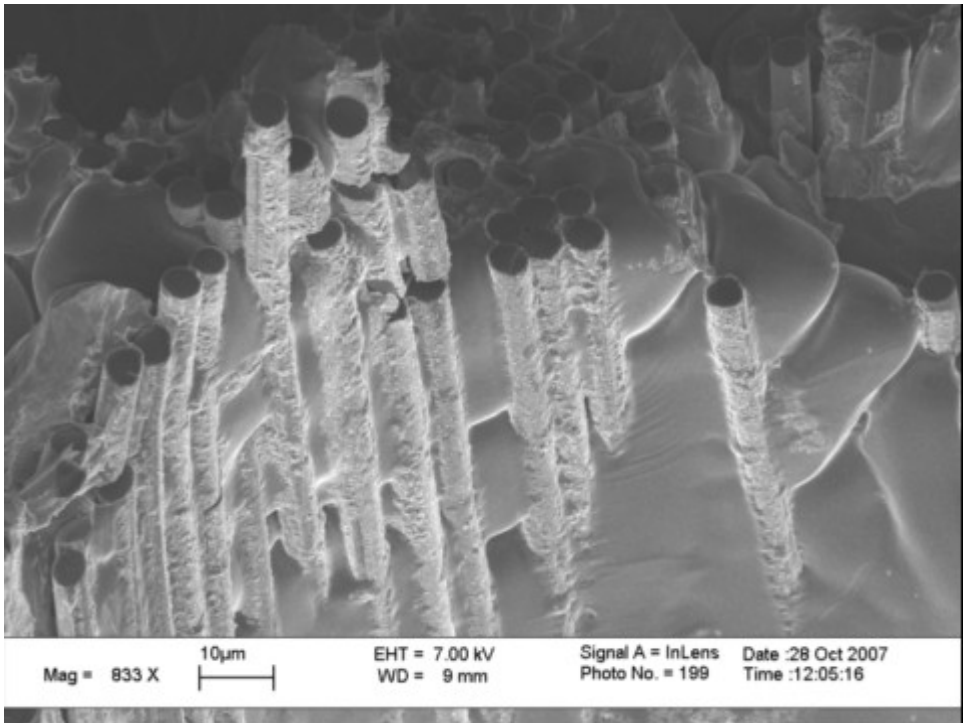

Figure 51: Coated fibers at the edge of a bubble.

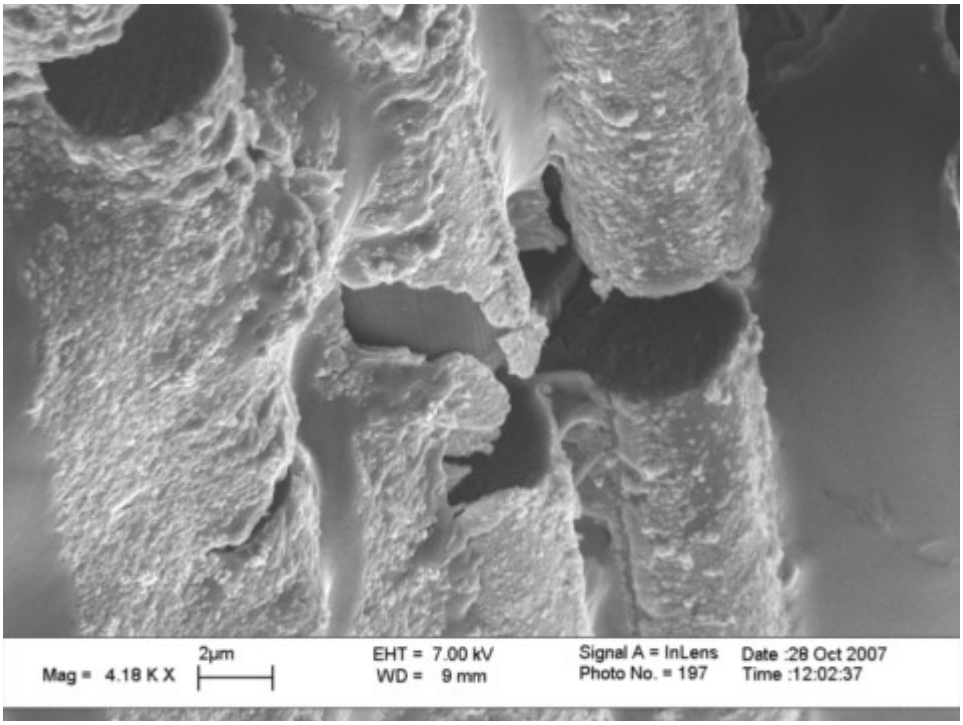

Figure 52: Fibers at the edge of bubble. Displays both poor coating adhesion (center) and fiber coating washing away in to matrix (left)

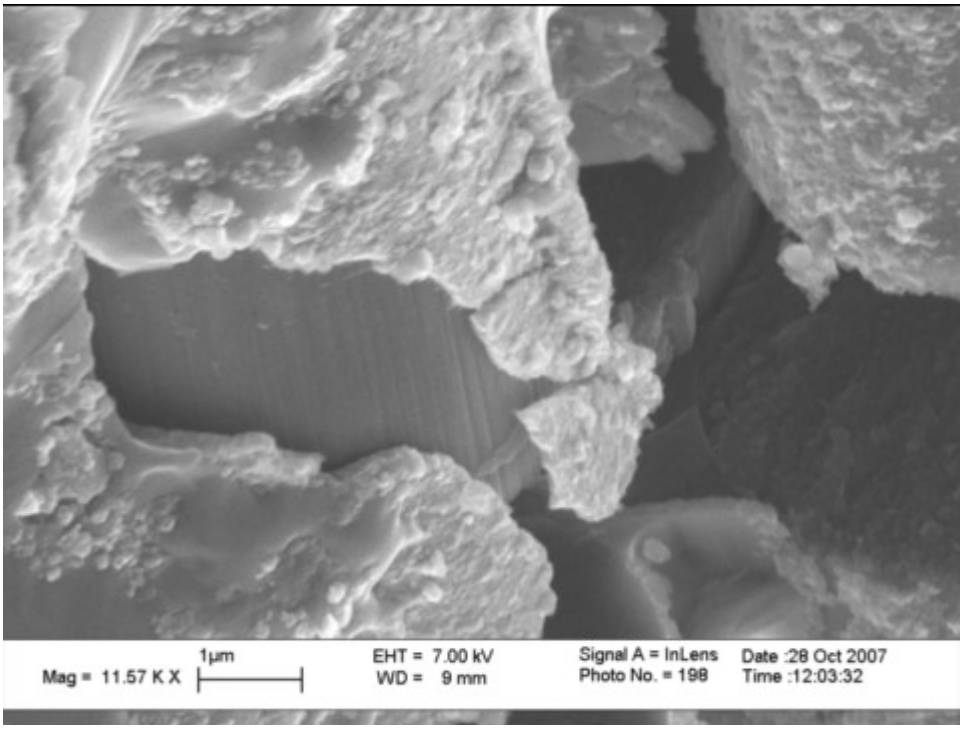

Figure 53: Detail of cracked and partially removed aluminum oxide coating from asphalt-coated fiber. Aluminum can be seen to the left of the fiber, mixing with the coating.

In general, the asphalt coating was unable to accomplish its singular task of improving oxide coating adhesion to the carbon fiber. Such a result is not wholly unsurprising, given that the coating was originally developed for composites produced by dip-coating of fibers in to the matrix. Despite not being able to withstand the ultrasound environment, the coating did have the side effect of improving the carbon fiber/aluminum matrix interface strength. Because the asphalt coating is composed more reactive carbon than the fiber, this interface strength improvement is likely the result of aluminum carbide formation. Although this would be deleterious to mechanical properties in large quantity, a coating of 20 nm in thickness uniformly covering 12,000 fiber filaments creates only 0.2 vol. % of reactive carbon. This fraction should not be significant compared to bubble volumes of 23%.

5. CONCLUSIONS

The research conducted in this program did not fully go as expected. Work by other groups indicating high %ROM properties using certain methods was not reproducible, and the many setbacks led to some frustration. In the end, the research was designed to determine a suitable low-cost coating for carbon fibers that would protect the fibers from interfacial reaction with aluminum and/or improve its wetting characteristics. Unfortunately, the fibers were nonreactive to the point that neither a baseline amount of carbide formation could be determined nor could oxide coatings, designed to inhibit that reaction, even adhere to the fiber surface. Of the several coatings that were developed, the one that came closest to improving any aspect of composite manufacture as compared to using bare fibers was the asphalt-based coating. This coating came about at such a time that it unfortunately received the smallest amount of research attention.

The high point of the research was the development of the continuous ultrasonic infiltration process, per one of the original objectives. Although it seemed to remove the oxide coatings, it was capable of producing well-infiltrated samples, even if the fibers within those samples were bare. Many of the other fabrication methods, such as squeeze-casting or dip-coating had not even partially worked.

6. RECOMMENDATIONS

The two biggest problems in fabrication of the composite samples were the amount of entrapped gases and the irregular sample shape. Passing the fibers through a vacuum, or perhaps even an ultrasonic cleanser would likely contribute significantly to reducing the porosity of the samples. Die drawing, either with a heated die, or as a post-processing step whereby the composites are heated to the softening temperature of aluminum and then drawn would produce uniform samples. Both of these steps would eliminate many of the unknown variables behind the poor mechanical properties of the composite samples.

It would perhaps be wise to look further in to the zirconia coating, as it is possible that it would be a more stable oxide than aluminum oxide at common composite processing temperatures. Magnesia and calcia are also interesting coating possibilities, since they are somewhat ductile and not reducible by aluminum. In general though, since the aluminum oxide coating displayed poor adhesion even after functionalizing the fiber surface, perhaps the most promising coating process would be a combination of the amorphous carbon coating coupled with a liquid metal transfer agent coating. With this combination, an adherent carbide coating could be produced without degrading the fiber. As stated previously, results from studies employing liquid metal transfer agent show great potential.

The one drawback of using such a coating is that it is conductive. This, however, remains an unknown, as these composites have not been evaluated for any sort of

environmental durability. It is possible that covering the interfaces, such coating the composites with an extra layer of aluminum, is sufficient corrosion protection. As well, since these composites have many potential high-temperature applications, it is possible that a mobile electrolyte will almost never be present if these materials are used at temperatures exceeding the boiling point of water.

REFERENCES

1: *ASM Metals Handbook*. ASM International: Metals Park, OH. 1993.

2: D.M. Goddard, P.D. Burke, and D.E. Kizer, "Continuous Graphite Fiber MMCs," *Engineered Materials Handbook*, vol. 1, pp. 867-873. 1987.

3: P. Shen, H. Fujii, T. Matsumoto, K. Nogi, "Critical Factors Affecting the Wettability of Alpha-Alumina by Molten Aluminum," *Journal of the American Ceramic Society*, vol. 87, pp. 2151-2159. 2004.

4: M. Naka, Y. Hirono and I. Okamoto, "Wetting of Alumina by Molten Aluminum and Aluminum-Copper Alloys," *Transactions of JWRI*, vol. 13, pp. 201-206. 1984.

5: Y.V. Naidich, Y.N. Chunvashov, N.F. Ishchuk and V.P. Krasovski, "Wetting of Some Nonmetallic Materials by Aluminum," *Poroschk. Metallurgia*, vol. 6, pp. 67-69. 1983.

6: O. Yamamoto, T. Sasamoto and M. Inagaki, "Effect of mullite coating film on oxidation resistance of carbon materials with SiC-gradient," *Journal of Materials Science letters*, vol. 19, pp. 1053-1055. 2000.

7: F. Delannay, L. Froyen, and A. Deruyttere, "The wetting of solids by molten metals and its relation to the preparation of metal-matrix composites," *Journal of Materials Science*, vol. 22, pp. 1-16. 1987.

8: J.P. Rocher, J.M. Quenisset, and R. Naslain, "Wetting improvement of carbon or silicon carbide by aluminum alloys based on a K2ZrF6 surface treatment: application to composite material casting," *Journal of Materials Science*, vol. 24, pp. 2697-2703. 1989.

9: G. Girot, J.P. Rocher, J.M. Quenisset, R. Naslain, in E-MRS Meeting, Fall, 1985.

10: S.-H Li, and C.-G. Chao, "Effects of Carbon Fiber/Al Interface on Mechanical Properties of Carbon-Fiber-Reinforced Aluminum-Matrix Composites," *Metallurgical and Materials Transactions*, vol. 35A, pp. 2153-2160. 2004.

11: M.H. Vidal-Setif, M. Lancin, C. Marhic, R. Valle, J.-L. Raviart, J.-C. Daux, and M. Rabinovitch, "On the role of brittle interfacial phases on the mechanical properties of carbon fibre reinforced Al-matrix composites," *Materials Science and Engineering A*, vol. 272, pp. 321-333. 1999.

12: J.W. Jung and S.H. Kang, "Advances in Manufacturing Boron Carbide-Aluminum Composites," *Journal of the American Ceramic Society*, vol. 87, pp. 47-54. 2004.

13: H.L. Cox, "The elasticity and strength of paper and other fibrous materials," *British Journal of Applied Physics*, vol. 3, pp. 72-79. 1952.

14: M. Vedula, R.N. Pangborn and R.A. Queeney, "Fiber anisotropic thermal expansion and residual thermal stress in a graphite/aluminum composite," *Composites*, vol. 19, pp. 55-60. 1988.

15: H. Hu, "Squeeze casting of magnesium alloys and their composites," *Journal of Materials Science*, vol. 33, pp. 1579-1589. 1998.

16: P.K. Rohatgi, D. Nath, and Z. Shi, "Coating of Copper on Graphite Fibers," *Zeitschrift für Metallkunde*, vol. 82, pp. 763-765. 1991.

17: J.F. Silvain, A. Proult, M. Lahaye, J. Douin, "Microstructure and chemical analysis of C/Cu/Al interfacial zones," *Composites: Part A*, vol. 34, pp. 1143-1149. 2003.

18: Y.-Q. Wang and B.-L. Zhou, "Behaviour of coatings on reinforcements in some metal matrix composites," *Composites: Part A*, vol. 27, pp. 1139-1145. 1996.

19: R.S. Bushby and V.D. Scott, "Evaluation of Aluminum-Copper Alloy Reinforced with Pitch-Based Carbon Fibers," *Composites Science and Technology*, vol. 57, pp. 119-128. 1997.

20: H.M Cheng, Z.H. Lin, B.L. Zhou, Z.G. Zhen, K. Kobayashi, and Y. Uchiyama, "Preparation of carbon fibre reinforced aluminium via ultrasonic liquid infiltration technique," *Materials Science and Technology*, vol. 9, pp. 609-614. 1993.

21: Y. Ono, "Ultrasonic Techniques of Imaging and Measurements in Molten Aluminum," *IEEE Transactions on Ultrasonics, Ferroelectrics and Frequency Control*, vol. 50, pp. 1711-1721. 2003.

22: K. Hynynen, N. McDannold, H. Martin, F.A. Jolesz, and N. Vykhodtseva, "The Threshold for Brain Damage in Rabbits Induced by Bursts of Ultrasound in the Presence of an Ultrasound Contrast Agent (Optison)," *Ultrasound in Medicine and Biology*, vol. 29, pp. 473-481. 2003.

23: B. Volker, *Practical Ship Hydrodynamics*. Elsevier: Oxford. 1999.

24: L.L. Shreir, R.A. Jarman and G.T. Burstein, eds., *Corrosion*, vol. 1. Elsevier: Oxford. 1994.

25: T. Matsunaga, K. Matsuda, T. Hatayama, K. Shinozaki and M. Yoshida, "Fabrication of continuous carbon fibre-reinforced aluminum-magnesium alloy composite wires using ultrasonic infiltration method," *Composites: Part A*, vol. 38, pp. 1902-1911. 2007.

26: J.B. Friler, A.S. Argon and J.A. Cornie, "Strength and toughness of carbon fiber reinforced aluminum matrix composites," *Materials Science and Engineering A*, vol. 162, pp. 143-152. 1993.

27: X. Zhenhai, M. Zhiying and Z. Yaohe, "Effect of Fibre Distribution on Infiltration Processing and Fracture Behaviour of Carbon Fibre-Reinforce Aluminum Composites," *Zeitschrift für Metallkunde*, vol. 82, pp. 766-768. 1991.

28: J.T. Blucher, U. Narusawa, M. Katsumata, A. Nemeth, "Continuous manufacturing of fiber-reinforced metal matrix composite wires - technology and product characteristics," *Composites: Part A*, vol. 32, pp. 1759-1766. 2001.

29: US Patent #6629557: Method and Apparatus for Manufacturing Composite Materials. Granted Oct 7, 2003.

30: 29 CFR 1915.172: Portable air receivers and other unfired pressure vessels.

31: B.C. Pai, G. Ramani, R.M. Pillai, and K.G. Satyanarayana, "Role of magnesium in cast aluminum alloy matrix composites," *Journal of Materials Science*, vol. 30, pp. 1903-1911. 1995.

32: Y. Kimura, Y. Mishima, S. Umekawa and T. Suzuki, "Compatibility between carbon fiber and binary aluminum alloys," *Journal of Materials Science*, vol. 19, pp. 3107-3114. 1984.

33: A.A. Zabolotsky, "Structure and properties formation of metal matrix composites," *Composites Science and Technology*, vol. 45, pp. 233-240. 1992.

34: X. Chen, G. Zhen, Z. Shen, "A TEM study of the interfaces and matrices of SiC-coated carbon fibre/aluminum composites made by the K2ZrF6 process," *Journal of Materials Science*, vol. 31, pp. 4297-4302. 1996.

35: M.K. Shorshorov, V.P. Alekhin, S.M. Savvateeva, V.B. Fedorov and T.A. Chernyshova, "Plasticizing and Wettability-Enhancing Coatings on Carbon, Silicon Carbide and Boron Fibers," *Thin Solid Films*, vol. 54, pp. 279-293. 1978.

36: T. Etter, M. Papakyriacou, P. Schulz and P.J. Uggowitzer, "Physical Properties of Graphite/Aluminum Composites Produced by Gas Pressure Infiltration Method," *Carbon*, vol. 41, pp. 1017-1024. 2003.

37: W.C. Harrigan, Jr. and R.H. Flowers, in Failure Modes in Composites IV: TMS/AIME Joint Composite Materials Committee Symposium, Oct, 1977.

38: J. Rams, A. Urena, M.D. Escalera, M. Sanchez, "Electroless nickel coated short carbon fibers in aluminum matrix composites," *Composites: Part A*, vol. 38, pp. 566-575. 2007.

39: S. Abraham, B.C. Pai, K.G. Satyanarayana and V.K. Vaidyan, "Studies on nickel coated carbon fibers and their composites," *Journal of Materials Science*, vol. 25, pp. 2839-2845. 1990.

40: A.G. Kulkarni, B.C. Pai and N. Balasubramanian, "The cementation technique for coating carbon fibers," *Journal of Materials Science*, vol. 14, pp. 592-598. 1979.

41: J.F. Silvain, J.M. Heintz, M. Lahaye, "Interface analysis in Al and Al alloys/Ni/carbon composites," *Journal of Materials Science*, vol. 35, pp. 961-965. 2000.

42: S. Abraham, B.C. Pai, K.G. Satyanarayana and V.K. Vaidyan, "Copper coating on carbon fibres and their composites with aluminum matrix," *Journal of Materials Science*, vol. 27, pp. 3479-3486. 1992.

43: T.P.D. Rajan, R.M. Pillai and B.C. Pai, "Reinforcement coatings and interfaces in aluminum metal matrix composites," *Journal of Materials Science*, vol. 33, pp. 3941-3503. 1998.

44: B. Wielage and A. Dorner, "Corrosion studies on aluminum reinforced with uncoated and coated carbon fibers," *Composites Science and Technology*, vol. 59, pp. 1239-1245. 1999.

45: T.A. Utigard, K. Friesen, R.R. Roy and J. Lim, "The properties and uses of fluxes in molten aluminum processing," *JOM*, vol. 50, pp. 38-43. 1998.

46: S.N. Patankar, V. Gopinathan, P. Ramakrishnan, "Processing of carbon fibre reinforced aluminum composite using K2ZrF6 treated carbon fibers: a degradation study," *Journal of Materials Science Letters*, vol. 9, pp. 912-913. 1990.

47: T.G. Nieh and A.E. Vidoz, "Carbide coatings on graphite fibers by liquid metal transfer agent method," *Journal of the American Ceramic Society*, vol. 65, pp. 227-230. 1982.

48: D.D. Himbeault, R.A. Varin and K. Piekarski, "Tensile properties of titanium carbide coated carbon fibre-aluminum alloy composites," *Composites*, vol. 20, pp. 471-477. 1989.

49: L.C. Klein, ed., *Sol-Gel Technology for Thin Films, Fibers, Preforms, Electronics and Specialty Shapes*. Noyes: Park Ridge, New Jersey. 1988.

50: H.A. Katzman, "Fibre coatings for the fabrication of graphite-reinforced magnesium composites," *Journal of Materials Science*, vol. 22, pp. 144-148. 1987.

51: P. Peng, X.D. Li, G.F. Yuan, W.Q. She, F. Cao, D.M. Yang, Y. Zhuo, J. Liao, S.L. Yang and M.J. Yue, "Aluminum oxide/amorphous carbon coatings on carbon fibers,

prepared by pyrolysis of an organic-inorganic hybrid precursor," *Materials Letters*, vol. 47, pp. 171-177. 2001.

52: Q.B. Zeng, "Fabrication of Al2O3-coated carbon fiber-reinforced Al-matrix composites," *Journal of Applied Polymer Science*, vol. 70, pp. 177-183. 1998.

53: J.P. Clement, H.J. Rack, K.T. Wu and H.G. Spencer, "Interfacial modification in metal matrix composites by the sol-gel process," *Materials and Manufacturing Processes*, vol. 5, pp. 17-33. 1990.

54: EPA, Office of Solid Waste and Emergency Response, List of lists: Consolidated list of chemicals subject to the Emergency Planning and Community Right-To-Know Act and section 112(r) of the Clean Air Act: CERCLA Hazardous Substances,

55: H.A. Katzman, "Fiber coatings for composite fabrication," *Materials and Manufacturing Processes*, vol. 5, pp. 1-15. 1990.

56: C. Geiculescu, H.G. Spencer, H.J. Rack, B. Sullivan, "Aqueous Sol-Gel Coating of Pitch-Based Graphite Fibers for Inclusion in Aluminum Matrix Composites," *Materials and Manufacturing Processes*, vol. 14, pp. 489-507. 1999.

57: M.I.F. Macedo, C.C. Osawa, C.A. Bertran, "Sol-Gel Synthesis of Transparent Alumina Gel and Pure Gamma Alumina by Urea Hydrolysis of Aluminum Nitrate," *Journal of Sol-Gel Science and Technology*, vol. 30, pp. 135-140. 2004.

58: J. Li, Y. Pan, C. Xiang, Q. Ge, and J. Guo, "Low Temperature Synthesis of Ultrafine Alpha-Alumina Powder by a Simple Aqueous Sol-Gel Process," *Ceramics International*, vol. 32, pp. 587-591. 2006.

59: P.K. Mallick, *Fiber-Reinforced Composites*. Marcel Dekker: New York. 1993.

60: M. De Sanctis, S. Pelletier and Y. Bienvenu, "On the formation of interfacial carbides in a carbon fibre-reinforced aluminum composite," *Carbon*, vol. 32, pp. 925-930. 1994.

61: M. Yang and V.D. Scott, "Carbide formation in a carbon fibre reinforced aluminum composite," *Carbon*, vol. 29, pp. 877-879. 1991.

62: V.B. Guthrie, ed., *Petroleum Products Handbook*. McGraw-Hill: New York. 1960.

63: US Patent #4376804: Pyrolyzed pitch coatings for carbon fiber. Granted Mar 15, 1983.